

5-2016

Development of a novel device for ventricular assist device outflow graft anastomosis.

Young Choi
University of Louisville

Follow this and additional works at: <https://ir.library.louisville.edu/etd>

Part of the [Biomedical Engineering and Bioengineering Commons](#)

Recommended Citation

Choi, Young, "Development of a novel device for ventricular assist device outflow graft anastomosis." (2016). *Electronic Theses and Dissertations*. Paper 2370.
<https://doi.org/10.18297/etd/2370>

This Master's Thesis is brought to you for free and open access by ThinkIR: The University of Louisville's Institutional Repository. It has been accepted for inclusion in Electronic Theses and Dissertations by an authorized administrator of ThinkIR: The University of Louisville's Institutional Repository. This title appears here courtesy of the author, who has retained all other copyrights. For more information, please contact thinkir@louisville.edu.

DEVELOPMENT OF A NOVEL DEVICE FOR VENTRICULAR ASSIST DEVICE
OUTFLOW GRAFT ANASTOMOSIS

By

Young Choi
B.S., University of Louisville, 2014

A Thesis
Submitted to the Faculty of the
University of Louisville
J. B. Speed School of Engineering
as Partial Fulfillment of the Requirements
for the Professional Degree

MASTER OF ENGINEERING

Department of Bioengineering

May 2016

DEVELOPMENT OF A NOVEL DEVICE FOR VENTRICULAR ASSIST DEVICE
OUTFLOW GRAFT ANASTOMOSIS

Submitted by: _____
Young Choi, B.S.

A Thesis Provided on

(Date)

By the following Reading and Examination Committee:

Steven C. Koenig, Ph.D., Thesis Director

Mark S. Slaughter, M.D.

Kevin M. Walsh, Ph.D.

Guruprasad A. Giridharan, Ph.D.

Kevin G. Soucy, Ph.D.

DEDICATION

This thesis is dedicated to my parents,

Kyung-Ju Choi

and

Jung-In Choi

ACKNOWLEDGMENTS

I thank Dr. Mark Slaughter and Dr. Steven Koenig for the opportunity to participate in this rewarding project. I also thank Dr. Guruprasad Giridharan, Mike Sobieski and Dr. Kevin Soucy for their continuous advice and guidance. This project would not have been possible without the support of the staff and students of the Advanced Heart Failure Research (AHFR) group at the Cardiovascular Innovation Institute: Cary Woolard, Todd Adams, Yu Wang, Abhinav Kanukunta, Peter Chen, and Landon Tompkins. I also thank Dr. Michele Gallo for the provision of excellent surgical support. Lastly, I thank the members of my thesis committee that have challenged me to critically evaluate my own work and uphold high-quality of scientific work: Dr. Steven Koenig, Dr. Mark Slaughter, Dr. Kevin Walsh, Dr. Guruprasad Giridharan, and Dr. Kevin Soucy. The experiences and knowledge I have gained working with the AHFR for the last four years are invaluable to my future career in medical device development. You all have driven me to question conventional thinking, challenge my own capabilities, and persist through adversity, which has ultimately served to help me develop personally, professionally, and academically. I am sincerely grateful to this group of individuals as they have opened many prestigious opportunities for my future.

ABSTRACT

Purpose: Left ventricular assist device (LVAD) therapy can be life-saving for advanced heart failure patients. Conventional anastomosis (surgical connection) of LVAD outflow grafts to the aorta requires aortic clamping and hand-suturing. Aortic clamping increases the risk for neurological complications. Hand-suturing may be time-consuming and requires significant surgical dexterity. There is currently no commercially available device for sutureless anastomosis of large vascular grafts (diameter > 5mm). To overcome these limitations, a prototype LVAD outflow graft anastomosis device (GrAD) that facilitates sutureless anastomosis was developed and tested to demonstrate proof-of-concept and feasibility for (1) secured attachment withstanding physiological pressures, and (2) comparable attachment strength to conventionally hand-sewn sutured anastomosis.

Methods: To demonstrate proof-of-concept, prototype GrADs were fabricated using a nitinol wire connector attached to a 15 mm graft, felt flanged cuff, and cyanoacrylate adhesive. To demonstrate feasibility, the GrAD was anastomosed to bovine descending aorta and tested in a mock flow loop over a range of static (0, 50, 100, 150, 200 mmHg) and dynamic pressures (normal, hypertension, heart failure, LVAD support) to quantify

leakage. The maximum pull-out force for the GrAD and sutured anastomosis were also measured after completing static and dynamic testing in the mock flow loop model.

Results: The GrAD remained securely attached during all static and dynamic pressure test conditions as evidenced by minimal leak rates during clinically equivalent normal (22.1 ± 9.3 ml/min), hypertension (23.1 ± 10.1 ml/min), heart failure (16.4 ± 6.4 ml/min), and LVAD support (16.4 ± 4.3 mL/min) test conditions. Significantly larger leak rates at normal dynamic pressure (120/80 mmHg) between the GrAD and previously reported results for hand-sutured anastomosis were not observed. Differences in peak pull-out force between GrAD (43.57 ± 17.31 N) and hand-sutured anastomosis (63.48 ± 8.72 N) were statistically indiscernible (paired t-test, $p < 0.5$). No indications of device damage were observed.

Conclusion: A prototype GrAD enabling a sutureless, adaptable, and angled LVAD outflow graft anastomosis was developed with preliminary feasibility testing demonstrating proof-of-concept. The proposed LVAD outflow GrAD may facilitate surgical implant by eliminating the need for hand-suturing, decrease implant time, and increase reliability and reproducibility with the potential to improve patient outcomes.

TABLE OF CONTENTS

	<u>Page</u>
APPROVAL PAGE	i
DEDICATION	ii
ACKNOWLEDGEMENTS	iii
ABSTRACT	iv
LIST OF TABLES	viii
LIST OF FIGURES	x
I. BACKGROUND	1
A. Heart Failure	1
B. Left Ventricular Assist Device (LVAD)	3
1. Surgical Implantation of LVADs	5
2. Outflow Graft Anastomosis of LVAD	7
C. Sutureless Anastomosis	9
D. Devices for Sutureless Anastomosis	10
E. Surgical Adhesives	17
F. Device Design for LVAD Outflow Graft Anastomosis Device (GrAD)	20
1. Design Requirements for a LVAD Outflow GrAD	20
2. Design Considerations for LVAD Outflow GrAD	24
3. Graft-to-Vessel Connection	24
4. Materials	25
5. Biomechanical Properties	27

II. METHODS.....	29
A. Study Design	29
B. Prototype Design Development	31
C. Nitinol Connector Fabrication.....	31
1. Frame Construction.....	33
2. Shape Setting Nitinol	34
D. Felt Flanged Cuff Fabrication	36
E. Bovine Aorta Specimens	36
F. Static and Dynamic Pressure Testing	37
G. Pull-out Testing.....	40
H. Analysis Methods.....	42
III. RESULTS	43
A. Final Prototype Design.....	43
B. Static Pressure Testing	44
C. Dynamic Pressure Testing.....	46
D. Pull-out Testing.....	50
IV. DISCUSSION.....	53
A. Limitations	56
V. CONCLUSION	58
VI. REFERENCES	60
APPENDIX I: RAW AND ADDITIONAL DATA	79
APPENDIX II: STATISTICAL ANALYSIS	83
CURRICULUM VITAE.....	87

LIST OF TABLES

Table 1: Physiologic and mechanical design requirements for an LVAD outflow graft anastomosis device (GrAD).....	20
Table 2: Average and maximum wall thicknesses of ascending aorta. Large variability in wall thicknesses is shown based on sex, race, and age (Li et al., 2004).....	23
Table 3: Hemodynamic tuning parameters for each dynamic mock loop test condition..	39
Table 4: Mean \pm standard deviation of leak rates for static pressure tests.....	45
Table 5: Mean \pm standard deviations of hemodynamic parameter measurements calculated on a beat-to-beat basis for dynamic mock loop tests; arterial pressure (ArtP); aortic pressure (AoP); aortic flow (AoF); ventricular assist device flow (VADF); left ventricular assist device (LVAD)	47
Table 6: Mean \pm standard deviation leak rates for dynamic mock loop pressure tests; left ventricular assist device (LVAD)	48
Table 7: Specifications for typical suture types used for anastomosis; needle:suture diameter ratio (N:S Ratio); polytetrafluoroethylene (PTFE).....	49
Table 8: Static pressure test raw leak rate data	79
Table 9: Dynamic pressure test leak rate data.....	80
Table 10: Dynamic pressure test hemodynamic beat-to-beat raw calculations	81

Table 11: Pull-out force raw data.....82

LIST OF FIGURES

- Figure 1:** Number of heart transplants performed in North America, Europe and other countries as reported by the International Society for Heart & Lung Transplantation Transplant Registry (Stehlik et al., 2010)2
- Figure 2:** Number of left ventricular assist device (LVAD) and total artificial heart implants from 2006-2014 as reported by the Interagency Registry for Mechanically Assisted Circulatory Support Devices (Kirklin et al., 2014).....3
- Figure 3:** Images showing different surgical approaches for implanting left ventricular assist devices (LVADs). A) Median sternotomy used for conventional implantation of LVADs (Zucchetta et al., 2014), B) Less-invasive incisions used for implantations of LVADs, also showing standard locations for inflow cannulation to the left ventricular apex and outflow graft anastomosis to the ascending aorta (Gregoric et al., 2008)7
- Figure 4:** Diagram of an end-to-side anastomosis performed using a running suture technique (Baker, 2015)8
- Figure 5:** Timeline showing the chronological development of historical sutureless anastomosis devices (P. Tozzi, 2007)9

Figure 6: Photo of the first generation St. Jude Medical Symmetry Aortic Connector.

Aortic wall is compressed between internal and external struts. Connection with the vessel is achieved with vein hooks (P. Tozzi, 2007).....10

Figure 7: Photo showing occlusion of St. Jude Medical Symmetry Aortic Connector one-month after implantation due to intima hyperplasia onto the struts (P. Tozzi, 2007).....11

Figure 8: Drawings showing the Cardioventions CorLink device. A) CorLink device being loaded with a graft vessel inserted through the side of the insertion tool, vessel-end everted, and pins penetrating through the everted vessel (Bar-El et al., 2003), B) CorLink device deployed into the side of a vessel showing pins penetrating intima and struts compressing the exterior surface of the vessel (Riess et al., 2002).....12

Figure 9: Images of the PAS-Port proximal aortic connector. A) Integrated deployment and aortotomy tool, B) Loaded vessel being deployed onto the proximal aorta, C) PAS-Port connector after deployment onto the aortic wall showing compression of the vessel wall without penetration (Dohmen et al., 2011) ..13

Figure 10: Images of the Converge Coronary Anastomosis Coupler and the Cardica C-port anastomosis devices. A) Converge Coronary Anastomosis Coupler attached to an artery showing angled anastomosis through attachment of two coupled connectors (Boening et al., 2005), B) Cardica C-port anastomosis device showing angled anastomosis through stapling in a interrupted suture manner (P. Tozzi, 2007)14

Figure 11: Photograph showing the end-to-side version of the Vascular Join anastomosis device. End of a synthetic graft is fastened to the prosthesis and a saddle element is fastened on to the side of the target vessel through connection of hooks into the wall of the vessel (P. Tozzi, 2007)15

Figure 12: Drawing showing a hybrid mechanical and adhesive anastomosis device. Stainless steel ring has 4 hooks extended axially with thickening at the end that are elastic and can be bent for insertion. Vessel connection is consolidated by cyanoacrylate adhesive (P. Tozzi, 2007).....19

Figure 13: Diagram showing systolic movement of vessel edges at the anastomosis due to sutured anastomosis. Schematic shows the reduction in cross-section lumen at systole or higher pressure (P. Tozzi, 2007)22

Figure 14: Diagram showing experimental design consisting of static and dynamic pressure, and pull-out tests29

Figure 15: Photographs of various views of the prototype LVAD outflow graft anastomosis device (GrAD) consisting of a nitinol connector fastened to a 15 mm vascular graft and felt flanged cuff: A) Side-view, B) Top-view, C) Bottom-view, D) Top-view inside lumen of graft.....30

Figure 16: Photographs of preliminary fit studies of the nitinol connector within silicone tubing and bovine descending aorta specimens. A) Curved nitinol connector within silicone tubing showing curvature due to forces exerted by the tubing, B) Struts of a flat nitinol connector protruding out of the aorta due to rigidity of thick wire gages, C) Poor conformation of a flat nitinol connector to the inner lumen aortic wall that have the potential for causing complications32

Figure 17: Photographs of the nitinol connector frame fabrication. A) Mill used for boring holes according to template mounted onto copper slip coupling, B) Copper slip coupling used to create curved nitinol connectors, C) Steel plate used to create flat nitinol connectors	33
Figure 18: Photograph of candidate prototype nitinol connectors of various wire gauges, curved/flat members, and with/without loops	34
Figure 19: Photographs of 0.36 mm gauge nitinol connector providing smooth conformation to the inner lumen wall of a bovine descending aorta specimen	35
Figure 20: Photographs of prototype felt flanged. A) Sewn flanged cuff without silicone coating, B) Flanged cuff with 3 coats of silicone	36
Figure 21: Photograph showing experimental setup for static pressure testing	38
Figure 22: Photograph and block diagram showing experimental setup for dynamic mock loop pressure tests; systemic vascular resistance (SVR); left ventricular assist device (LVAD)	40
Figure 23: Experimental setup for pull-out testing	41
Figure 24: Dimensions of the prototype nitinol connector used for experimentation	43
Figure 25: Dimensions of the prototype flanged cuff used for experimentation.....	44
Figure 26: Leak rates for each vessel during static pressure tests. Vessel 2 consistently showed greater leak rates at all pressures ≥ 50 mmHg	45
Figure 27: Graphs comparing pressure and flows for each dynamic mock loop condition reflecting typical physiologic trends in hemodynamic parameters associated	

with each condition; arterial pressure (ArtP); aortic pressure (AoP); aortic flow (AoF); left ventricular assist device (LVAD)	46
Figure 28: Sample waveforms collected for normal, hypertension, heart failure, and LVAD support during dynamic mock loop tests.....	47
Figure 29: Leak rates for static and dynamic pressure tests; left ventricular assist device (LVAD)	49
Figure 30: Graph comparing mean leak rate from graft anastomosis device (GrAD) and literature reported leak rate of Hemo-Seal (HS), Prolene (PR 1, PR 2), and expanded-polytetrafluoroethylene (PTFE) sutures. Asterisks show significant differences between GrAD and PR1 and PTFE ($p < .05$)	50
Figure 31: Peak pull-out force for graft anastomosis device (GrAD) and sutured anastomosis	51
Figure 32: Photos of the graft anastomosis device (GrAD) after pull-out testing with no indications of device damage. A) The debonded device with an observable layer of adventitial tissue on the flanged cuff, 2) Bovine descending aorta after delamination of a portion of the adventitial tissue by the device.....	51
Figure 33: Photographs of the suture anastomosis after pull-out testing. A) Anastomosis site on the aorta where slits from suture ripping vessel can be observed, B) Fractured suture with a sliver of aortic tissue remaining	52

I. BACKGROUND

A. Heart Failure

Heart failure (HF) is a progressive condition in which the heart muscle loses its capacity to pump adequate blood volume to satisfy the body's demand for oxygen and nutrients, and removal of carbon dioxide and waste. It continues to be one of the largest unsolved medical complications despite being one of the most explored medical diseases. HF is the leading cause of death in the United States, affecting ~5.7 million people in the US with a projected increase in prevalence of 46% from 2012 to 2030 (Mozaffarian et al., 2015). In 2011, the direct and indirect costs of HF in the US was an estimated 34.4 billion dollars (Heidenreich et al., 2011), and is projected to increase from 44.6 to 97 billion from 2015 through 2030 (Roger et al., 2012). According to the National Center for Health Statistics (NCHS) and the National Heart, Lung, and Blood Institute (NHLBI), one in 9 deaths in the US have been attributed to HF. Although survival following HF diagnosis has improved over time due to advances in medical treatment, the death rate remains high with a ~50% mortality rate within 5 years of HF diagnosis (Levy et al., 2002; V. L. Roger et al., 2004).

Preferred treatment strategy(s) for HF is dependent on the type of HF and severity. For example, symptoms are managed using pharmacologic therapy and changes to lifestyle factors in early stage HF. Unfortunately, there is a large group of patients with severe HF (advanced HF) that are unresponsive to pharmacologic therapy and changes in lifestyle factors. The gold standard for treating these advanced HF patients is heart transplantation, but the supply of donor hearts cannot satisfy the clinical demand. In 2013, only 51.1% of candidates listed for heart transplantation received heart transplants (Colvin-Adams et al., 2014). The number of heart transplants has reached a plateau while the number of advanced HF patients continues to grow (Figure 1). Subsequently, there is a significant unmet clinical need and demand for alternative HF treatment options.

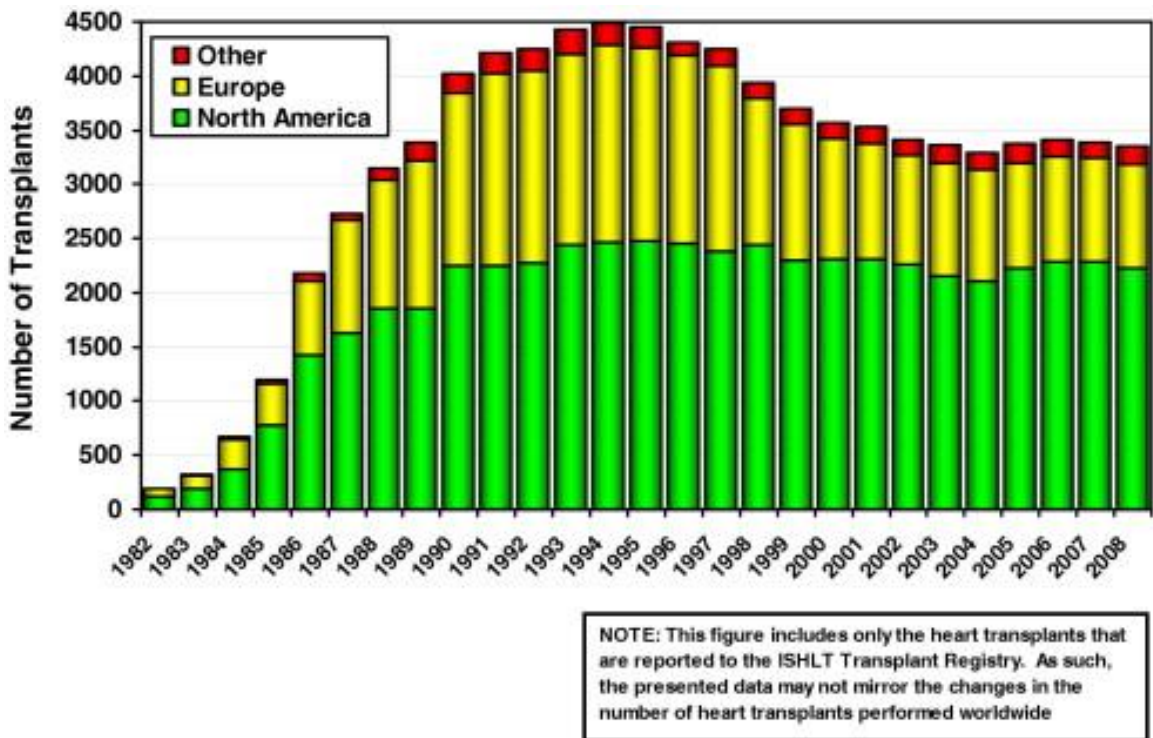


Figure 1: Number of heart transplants performed in North America, Europe and other countries as reported by the International Society for Heart & Lung Transplantation Transplant Registry (Stehlik et al., 2010).

B. Left Ventricular Assist Device (LVAD)

Left ventricular assist devices (LVADs) are blood pumps that assist the blood pumping function of the heart in advanced heart failure patients (Figure 2). In 2006, the Interagency Registry for Mechanically Assisted Circulatory Support Devices (INTERMACS) reported 94 LVAD implants per year, which increased to 2,447 LVAD implants per year in 2014 (Kirklin et al., 2015). LVADs were initially implanted as bridge to transplantation (BTT) devices for patients with deteriorating HF that were at high mortality risk while on the waiting list wait for a heart transplant. Due to early success and technical advances in LVAD technology over the past 15 years, the use of these devices has expanded to include long-term and myocardial recovery therapy.

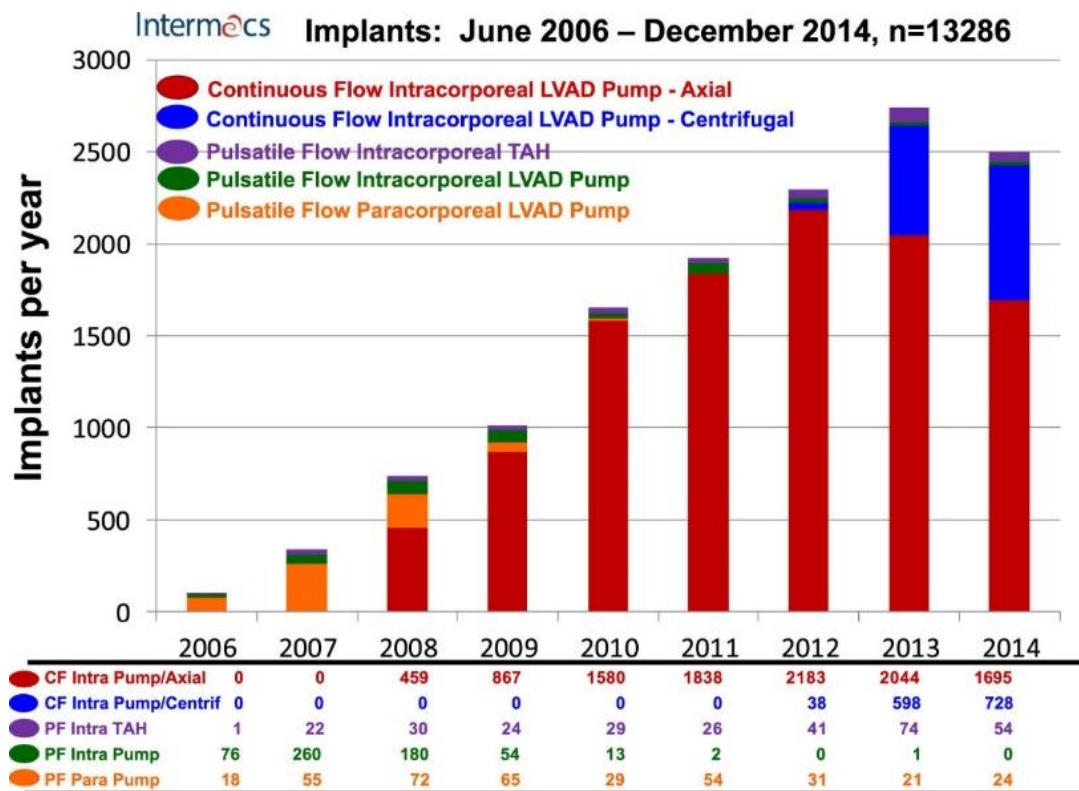


Figure 2: Number of left ventricular assist device (LVAD) and total artificial heart implants from 2006-2014 as reported by the Interagency Registry for Mechanically Assisted Circulatory Support Devices (Kirklin et al., 2014).

LVAD technology has evolved significantly from first-generation devices that were large, pulsatile, volume displacement pumps to current third-generation devices that are smaller size, lighter weight, valveless, and magnetically-levitated rotary pumps. Technological innovations of LVADs included miniaturization of pumps, increased durability due to less moving parts, introduction of continuous-flow pumps, and magnetically levitated pump rotors. In parallel with the technological evolution of LVADs, there has been a marked improvement in the survival rates after LVAD implantation. The one-year and two-year actuarial survival rates of these continuous-flow devices are 68% and 58%, respectively, compared to 55% and 24% for first generation pulsatile-flow devices (Slaughter et al., 2009). In addition, there have been significantly less clinically significant adverse events (e.g. device-related infection, non-device-related infection, right heart failure, respiratory failure, renal failure, cardiac arrhythmia) in patients with continuous-flow devices compared to pulsatile-flow devices (Slaughter et al., 2009).

The success of LVADs as BTT devices combined with increased survival rates and reduced adverse events has expanded their clinical role to permanent (long-term) support devices (destination therapy). The Randomized Evaluation of Mechanical Assistance for the Treatment of Congestive Heart (REMATCH) trial compared optimal medical management (pharmacological therapy) vs Heartmate I Left Ventricular Assist Device LVAD as permanent treatment among 129 advanced HF patients. The LVAD group had a 52% one-year survival and 23% two-year survival compared to 25% one-year survival and 8% for the optimal medical management (OMM) therapy (Rose et al.,

2001). These results from the REMATCH trial led to Food and Drug Administration (FDA) approval of a few CF LVADs for destination therapy (DT).

Clinical research has demonstrated improvements in cardiac function and reverse remodeling with LVAD support offering hope for LVAD use as a potential therapy strategy for sustained myocardial recovery (Frazier et al., 1996). Studies offer compelling evidence that chronic volume unloading provided by LVADs is associated with beneficial structural and molecular remodeling that may lead to functional improvement (Birks et al., 2005; Birks et al., 2006; Cullen et al., 2006; Hall et al., 2007; Latif, Yacoub, George, Barton, & Birks, 2007). For some patients, the reverse remodeling that occurs may allow for removal of the LVAD due to regained cardiac function (Birks, 2010; Birks et al., 2006; Dandel et al., 2005). Emma Birks et al. has pioneered the methodology of combining the neurohormonal effects of HF medications and mechanical left ventricular volume unloading with LVADs as a treatment strategy for myocardial recovery (Birks et al., 2006; Lenneman & Birks, 2014). This treatment method has allowed about 2/3 of a small cohort of patients receiving the treatment to regain cardiac function for device removal (Birks, 2010; Birks et al., 2006). Expanding clinical indications for LVAD therapy as BTT, DT, or myocardial recovery promotes a larger application and use of LVADs for HF patients.

1. Surgical Implantation of LVADs

Although LVADs can be a life-saving therapy for advanced HF patients, implantation of these devices requires a major surgical procedure that can take up to 4+ hours. Conventional implantation for popular LVAD systems in the US—Thoratec

HeartMate II, HeartWare HVAD, Jarvik-2000—require a median sternotomy (Figure 3), cardiopulmonary bypass (CPB) and partial clamping of the aorta. Median sternotomy is associated with risk of infection, high hospital stay costs, and severe burden for the patient (Graf et al., 2010; Heilmann et al., 2013; Taylor, Mitchell, & Mitchell, 2012). CPB is associated with post-operative bleeding (Ohri et al., 1991) and/or pulmonary complications (Huffmyer & Groves, 2015), as well as potential risk of blood damage (Mamikonian et al., 2014). Clamping of the aorta has been associated with increased risk of neurological complications (Zamvar et al., 2002) and aortic dissections (Stanger, Oberwalder, Dacar, Knez, & Rigler, 2002). These limitations have led investigators to investigate the development of alternative surgical approaches and/or novel technologies that may enable less-invasive implantation techniques to reduce time and facilitate surgery and recovery.

Several investigators have reported less-invasive (Figure 3) and beating heart (off-pump; without cardiopulmonary bypass) surgeries for LVAD implantation (Anyanwu, Fischer, Plotkina, Pinney, & Adams, 2007; Cheung et al., 2011; Frazier, 2003; Gregoric et al., 2008; Maltais, Davis, & Haglund, 2014; Rojas et al., 2015; Sun et al., 2008; Wagner et al., 2015). For example, the Sutureless Beating Heart connector (APK Advanced Medical Technologies, Atlanta, GA) allows for off-pump, beating heart implantation of inflow cannulas of LVADs (Koenig et al., 2014). The combination of less-invasive surgical approaches and novel technologies may enable less-invasive and off-pump implantation of LVADs, thereby potentially reducing post-operative recovery

times, cost of hospital stays, and the risk of further complications associated with CPB and median sternotomy.

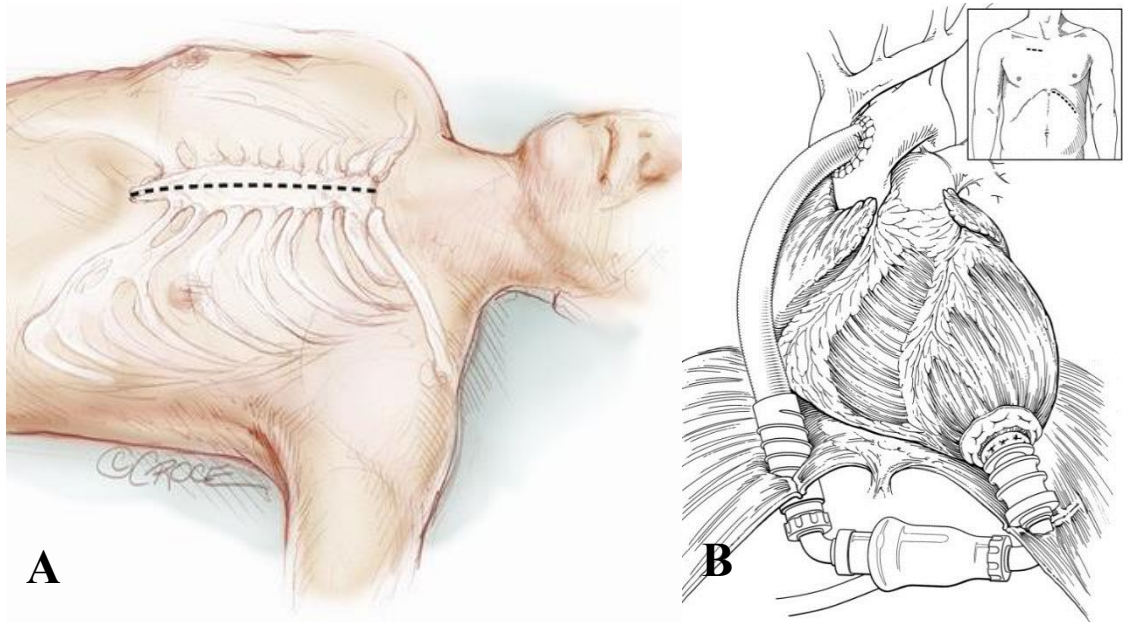


Figure 3: Images showing different surgical approaches for implanting left ventricular assist devices (LVADs). A) Median sternotomy used for conventional implantation of LVADs (Zucchetta, Tarzia, Bottio, & Gerosa, 2014), B) Less-invasive incisions used for implantations of LVADs, also showing standard locations for inflow cannulation to the left ventricular apex and outflow graft anastomosis to the ascending aorta (Gregoric et al., 2008).

2. Outflow Graft Anastomosis of LVAD

To complete the LVAD outflow graft anastomosis (surgical connection), a side-biting clamp is placed on the ascending aorta to facilitate suturing and minimize blood loss by creating an area of flow stagnation. A small incision is then made to the aorta (aortotomy) to connect to outflow graft. An aortic punch is typically used to round out the edges of the incision to prevent damage or tearing at the incision site. A 3-0 to 5-0 Prolene suture is used to hand-suture a gelatin-impregnated, woven polyethylene terephthalate (PET) graft in a running suture technique (Figure 4). Upon completion of the suturing, the side-biting clamp is removed and blood flow provided through the outflow graft.

Conventional LVAD outflow graft anastomosis requires aortic cross- or partial-clamping, which as mentioned previously is associated with aortic complications. To complete anastomosis of the LVAD outflow graft to the aorta requires surgical dexterity and may be time-consuming (up to 30 minutes) to complete. As surgical implantation for LVADs advance toward less-invasive, off-pump procedures, alternative solutions are warranted for completing LVAD outflow graft anastomosis that would complement an altogether less-invasive procedure.

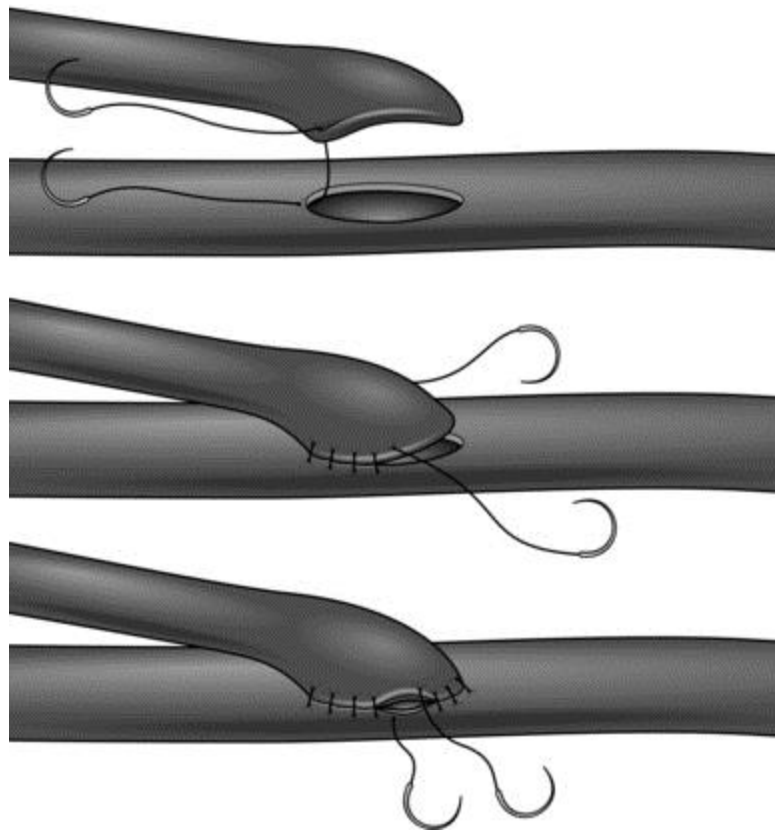


Figure 4: Diagram of an end-to-side anastomosis performed using a running suture technique (Baker, 2015).

C. Sutureless Anastomosis

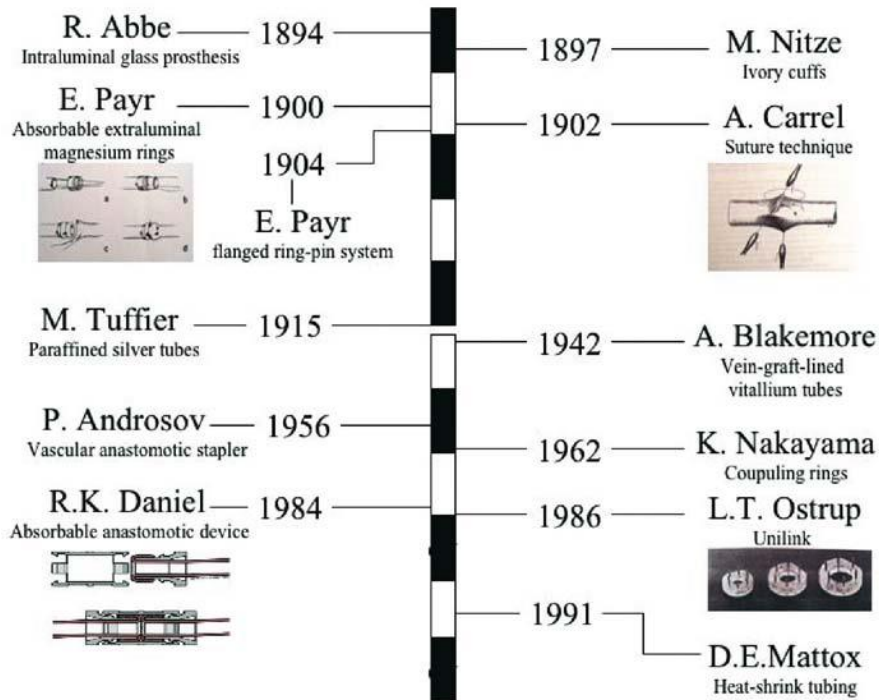


Figure 5: Timeline showing the chronological development of historical sutureless anastomosis devices (P. Tozzi, 2007).

Historically, anastomosis has been completed using hand-suture methods based on the principles established by Alexis Carrel in 1902 (Carrel, 1902). The reliability and long-term patency results of this method has rooted it as the gold standard for vascular anastomosis. Earliest scientific reports for completing sutureless anastomosis used crude materials (e.g. quill-pens, glass, ivory cuffs, ox shin bones) as vascular prostheses (Abbe, 1894; Callow, 1982; Muir, 1914; Nitze, 1897; Tuffier, 1915). More promising technologies were introduced in the 1900s that employed interlocking rings (Berggren, Ostrup, & Lidman, 1987; Nakayama, Tamiya, Yamamoto, & Akimoto, 1962; Payr, 1904), symmetrical anvils (Daniel & Olding, 1984), staples (Androsov, 1956), heat-shrink tubing (Mattox & Wozniak, 1991), and clips (Kirsch, 1998). Less mechanical approaches for sutureless anastomosis included the combination of lasers with stay stitches (Grubbs et al., 1988; Jain & Gorisch, 1979; Phillips et al., 1999). None of these

devices were widely accepted due to limitations that included complex and cumbersome instrumentation, rigid foreign bodies, and poor clinical results (P. Tozzi, 2007).

D. Devices for Sutureless Anastomosis

Currently there are no commercially available devices for sutureless anastomosis of large-diameter synthetic grafts (>5 mm), similar to those used for LVAD outflow grafts. The majority of devices enabling sutureless anastomosis were developed for facilitating coronary artery bypass graft (CABG) procedures, which require end-to-side anastomosis of small-diameter arteries/veins (<5 mm). These devices may be categorized as proximal (anastomosed to the ascending aorta) or distal (anastomosed to the descending aorta) anastomotic devices.

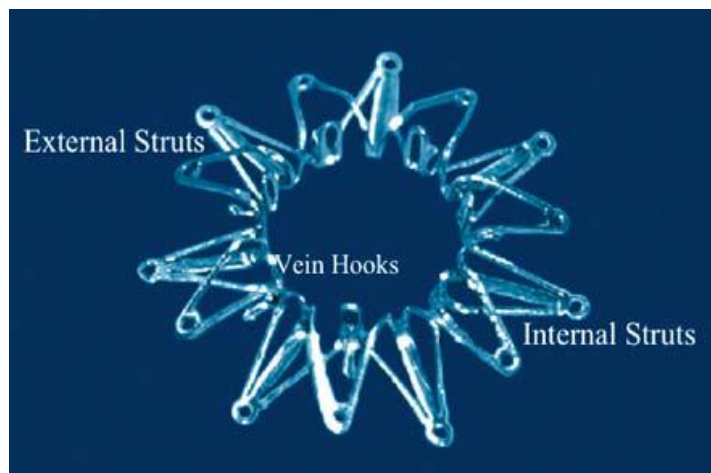


Figure 6: Photograph of the first generation St. Jude Medical Symmetry Aortic Connector. Aortic wall is compressed between internal and external struts. Connection with the vessel is achieved with vein hooks (P. Tozzi, 2007).

The St. Jude Medical Symmetry Aortic Connector was the first nitinol connector to gain clinical approval (P. Tozzi, 2007). Nitinol is a Nickel and Titanium alloy that exhibits superelastic and shape-memory properties enabling it to return to an original shape after large deformations. This star-shaped connector attaches vein grafts at a 90°

angle to the proximal aorta by compressing the aortic wall between internal and external struts (Figure 6). Once a graft vein is excised, it is loaded onto the delivery system. Hooks arranged around the inner ring of the connector fasten to the vein. A limitation of this device is that only a single end of the vessel can be anastomosed since a free-end is required for loading onto the deployment tool. Furthermore, the 90° take-off angle requires precise placement of the graft vessel to avoid graft kinking. Of the 44 anastomoses constructed by the Symmetry Aortic Connector 55% were occluded (Figure 7) at a mean follow-up period of 41 months (P. Bergmann et al., 2007). In another study, 74 patients underwent elective CABG in which 131 anastomoses were constructed using the Symmetry Aortic connector, in which 20 bypass grafts (2 hand suture, 18 Symmetry) showed severe stenosis or occlusion (Traverse et al., 2003). Although the Symmetry device reliably allows blood flow acutely through an anastomosis (Dewey et al., 2004; Eckstein et al., 2002), long-term clinical results discouraged the continued usage of the device.



Figure 7: Photograph showing occlusion of St. Jude Medical Symmetry Aortic Connector one-month after implantation due to intima hyperplasia onto the struts (P. Tozzi, 2007).

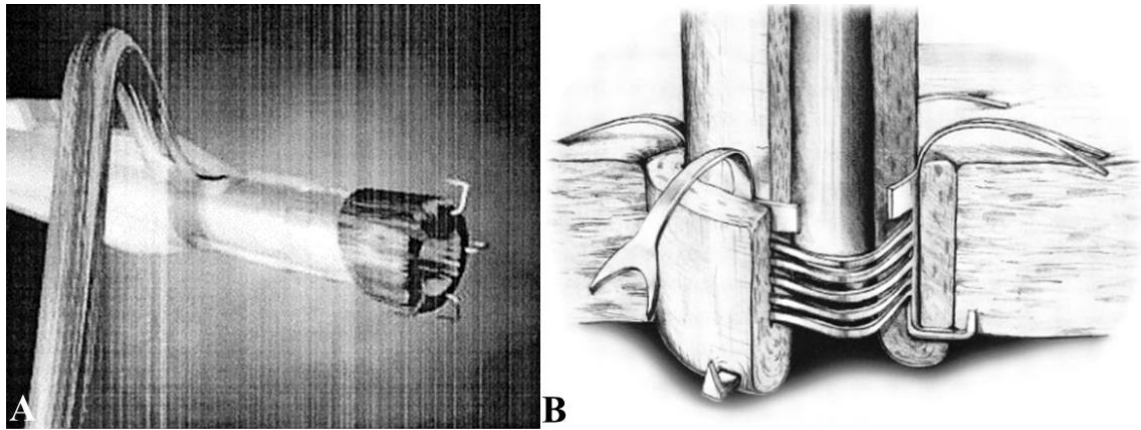


Figure 8: Drawings showing the Cardioventions CorLink device. A) CorLink device being loaded with a graft vessel inserted through the side of the insertion tool, vessel-end everted, and pins penetrating through the everted vessel (Bar-El, Tio, & Shofti, 2003), B) CorLink device deployed into the side of a vessel showing pins penetrating intima and struts compressing the exterior surface of the vessel (Riess et al., 2002)

Other devices that allow anastomosis between the ascending aorta and a graft vessel include the CorLink (Cardioventions, Somerville, NJ) and Spyder (Coalescent Surgical, Sunnyvale, CA). The CorLink is a nitinol connector that requires a graft vessel to be everted over the end of the connector, which may be cumbersome and/or damage the vessel intima (innermost cellular layer in contact with blood flow), as shown in Figure 8. The graft vessel is pulled through an insertion tool for deployment (Figure 8). The mechanism of loading the vessel through the side of the integrated deployment tool offers the advantage of not requiring the graft to have a free-end. For this device to successfully attach to a target vessel, two sets of five pins must fully-penetrate through the vessel. The Spyder uses a novel approach of depositing 6 nitinol sutures (U-clips) between a pre-mounted vein graft and the aorta, resulting in a connection similar to an interrupted suture technique without the requirement of tying knots. Both the Corlink and Spyder devices demonstrated higher incidence of occlusion versus standard suture anastomosis, as well as failed to create hemostasis upon deployment (Biancari et al., 2007; Gummert et al., 2007). These devices had limited foreign body exposure, but the

increased vascular injury from penetration of pins/clips may have alternatively triggered intimal hyperplasia (proliferation of intimal cells decreasing vessel lumen space) and gradual occlusion of the graft. These pre-clinical and clinical results failed to gain the enthusiasm for adoption of these devices, therefore these devices are no longer used clinically.

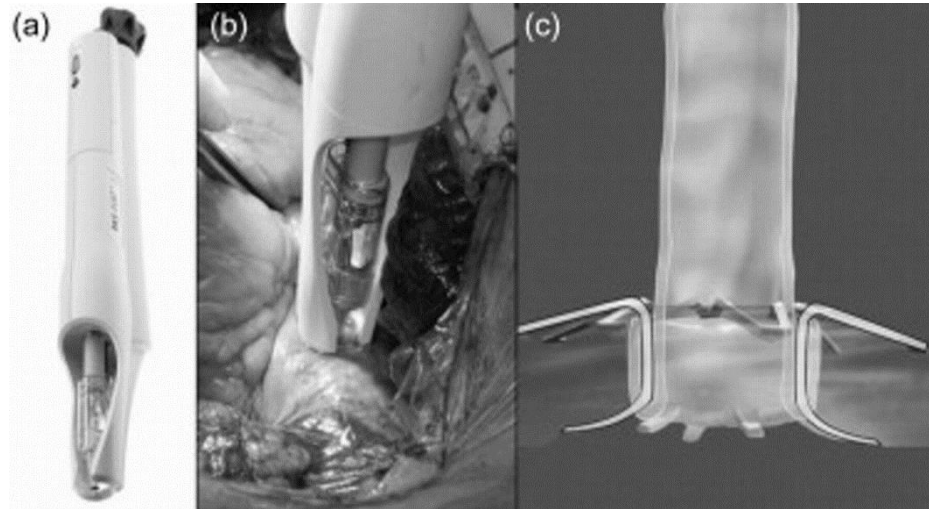


Figure 9: Images of the PAS-Port proximal aortic connector. A) Integrated deployment and aortotomy tool, B) Loaded vessel being deployed onto the proximal aorta, C) PAS-Port connector after deployment onto the aortic wall showing compression of the vessel wall without penetration (Dohmen et al., 2011).

The PAS-Port (Cardica Inc, Redwood City, CA) is the only commercially available proximal anastomosis system that is currently distributed in both Europe and the US (Figure 9). Unlike aforementioned devices, this novel device integrates the action of the aortotomy and deployment of the connector into a single tool. After loading the graft vessel onto the deployment tool, the tool is placed onto the target location and the surgeon rotates a knob on the tail-end of the tool to complete the anastomosis. In the pivotal EPIC trial, 220-patients requiring CABG with at least 2 vein grafts randomly received one graft with the PAS-Port device, and the other with a hand-sewn suture method. Results showed an 80.3% 9-month graft patency (state of being unblocked) versus 82.0% for hand-sewn. Similar freedom from major adverse cardiac events at 9-

months was demonstrated between the two methods. However, the PAS-Port system was associated with a statistically significant, 4.6 ± 3.9 minute reduction in anastomotic time from the overall 7.7 ± 2.9 minutes required to complete conventional hand-sewn anastomosis (Puskas et al., 2009). Promising mid- to long-term results were also demonstrated in Japan (Kai et al., 2009) and Europe (Gummert et al., 2006).

Technological innovations of the PAS-Port system include: 1) Integrated aortotomy and deployment tool, 2) Reduced non-biologic material exposure inside the vessel lumen, 3) Utilization of 316L stainless-steel material in replacement of nitinol. These characteristics may have contributed to the greater clinical results of PAS-Port system compared to preceding devices.

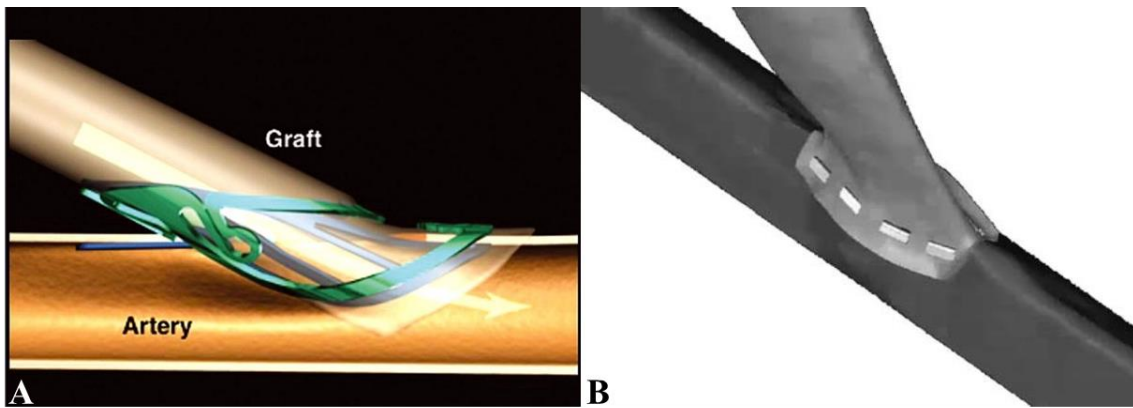


Figure 10: Images of the Converge Coronary Anastomosis Coupler and the Cardica C-port anastomosis devices. A) Converge Coronary Anastomosis Coupler attached to an artery showing angled anastomosis through attachment of two coupled connectors (Boening et al., 2005), B) Cardica C-port anastomosis device showing angled anastomosis through stapling in an interrupted suture manner (P. Tozzi, 2007).

The second category of sutureless anastomotic devices are intended for distal anastomosis. Some of the more promising distal anastomotic devices are the Converge Coronary Anastomosis Coupler (Converge Medical Inc., Sunnyvale, CA) and the Cardica C-Port (Cardica Inc., Redwood City, CA). The Converge device is a two-piece coupler made of nitinol that clamps the vessels being anastomosed together (Figure 10). The graft vessel is placed between the two frames, which is loaded into a dedicated deployment

tool for insertion into the target artery at a 30° take-off angle. Loading of the coupler has been reported to be cumbersome and anastomosis leak has been common (Boening et al., 2005). The C-port is an anastomosis device that deposits stainless steel staples to form an end-to-side anastomosis similar to an interrupted suture technique (Figure 10). In a single-center study, the anastomotic patency of the Cardica C-Port was compared to the hand-sew anastomosis. One-year patency rates between the two techniques showed no statistically discernible differences, and the incidence of complications was comparable to the hand-sewn anastomosis (Verberkmoes et al., 2013). The C-port is particularly promising because it creates an angled anastomosis, has similar non-intimal surface as a sutured anastomosis thereby requiring no anticoagulation therapy, and is capable of creating a side-to-end anastomosis in very small (1mm) diameter vessels (P. Tozzi, 2007).

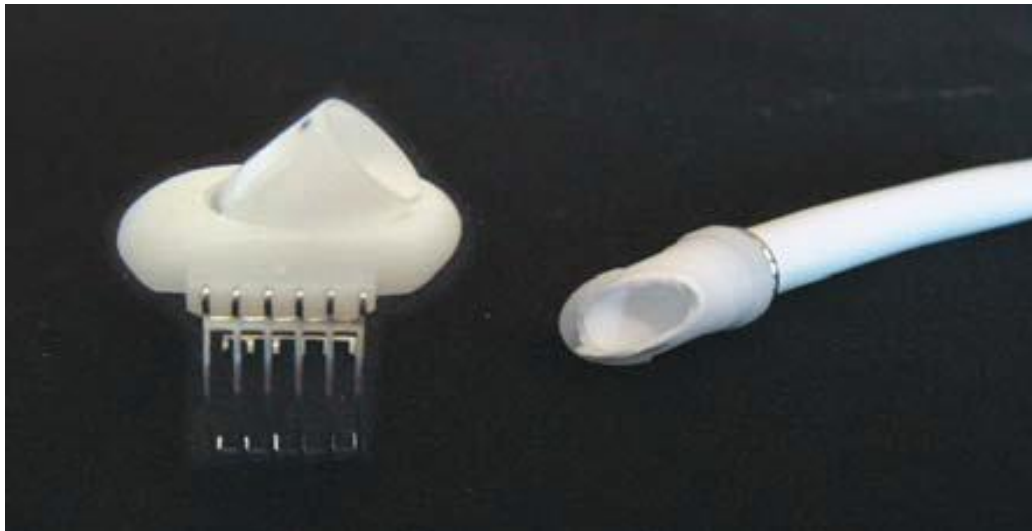


Figure 11: Photograph showing the end-to-side version of the Vascular Join anastomosis device. End of a synthetic graft is fastened to the prosthesis and a saddle element is fastened on to the side of the target vessel through connection of hooks into the wall of the vessel (P. Tozzi, 2007).

One of the most promising sutureless devices that addresses the limitations of vascular injury and foreign-body blood exposure is the Vascular Join (Idee & Sviluppo LLC, Bologna, Italy). The Vascular Join consists of two metallic rings that are fixed to

the exterior of either a biologic or synthetic graft (Figure 11). There are various sized elements accommodating 3 to 12 mm diameter grafts, but there are no restrictions in respect to vessel size. For end-to-side anastomosis, a saddle element is attached to the exterior of the desired side vessel by hooks that only penetrate the vessel wall without full-thickness penetration. After creation of an elliptical hole with a dedicated rotary blade, the graft with a pre-mounted ring is inserted to create the anastomosis. The device provides reproducible anastomosis with biologic and synthetic grafts with the advantages of zero foreign-body exposure to blood, angled geometry, and may be adapted to any size graft regardless of graft diameter and thickness. Clinical results for the end-to-end version of the Vascular Join showed 100% patency, immediate hemostasis, adequate blood flow and no instances of technical failure (Ferrari, Tozzi, & von Segesser, 2007). Long-term and end-to-side clinical studies are needed in order for this device to gain wide clinical acceptance.

All of the aforementioned devices, except the Vascular Join, are limited to applications of attaching small biologic vessels to either the ascending or descending aorta. None of these devices were designed for LVAD outflow grafts anastomosis, hence have not been tested in relevant models consisting of end-to-side anastomosis to a large aortotomy (>5 mm diameter) under turbulent and high pressures common to the ascending aorta. There are currently no commercially-available devices or scientific reports of sutureless anastomotic devices for LVAD outflow grafts, providing an opportunity for the development of innovative technologies to facilitate anastomosis of LVAD outflow grafts.

E. Surgical Adhesives

Surgical adhesives are a promising and growing area for development due to many potential clinical applications. Currently, octyl cyanoacrylate (Dermabond) is in use clinically to replace sutures for incisional or laceration closure (Bruns & Worthington, 2000). Other adhesives, such as fibrin sealants (e.g. EVICEL, TISSEAL), are clinically approved as an adjunct to standard sutures for hemostasis. Fibrin adhesives have shown to be highly effective in preventing leaks in conjunction with sutures for vessel-to-vessel anastomosis, as well as synthetic graft-to-vessel anastomosis (Saha et al., 2012). In the application of wound closure, adhesives offer the advantage of fast application, less traumatic closure, and the ability for application within difficult working environments.

Many hemostatic adhesives have been developed based on fibrin, collagen, cyanoacrylate (Hee Park et al., 2003; Szanka, Szanka, Şen, Nugay, & Kennedy, 2015), polyethylene glycol (Marc et al., 2000), albumin-glutaraldehyde (Küçükaksu, Akgül, Çağlı, & Taşdemir, 2000; Mitrev, Belostotskii, & Hristov, 2007), or gelatin-resorcinal-formaldehyde (Perrin et al., 2009). Other adhesives have drawn inspiration from nature, such as citrate-based mussel-inspired adhesive (Mitrev et al., 2007), and poly(glycerol sebacate acrylate)-based gecko-inspired adhesive (Mahdavi et al., 2008). Requirements of an ideal hemostatic surgical adhesive is that it must be easy to use, safe, polymerize in a wet environment, and have strong adhesion properties. Development of a strong hemostatic adhesive with these properties has the potential of replacing sutures.

Several studies have attempted replacement of sutures with available hemostatic adhesives. Fibrin- and cyanoacrylate-based adhesives has been used to complete microvascular anastomosis (Carton, Heifetz, & Kessler, 1962; Carton, Kessler, Seidenberg, & Hurwitt, 1960; Carton, Kessler, Seidenberg, & Hurwitt, 1961; Ikossi-O'Connor, Ambrus, & Rao, 1983; Kim et al., 2004). However, fibrin adhesives are inherently weak adhesives and has not been reported to be used alone in high pressure arterial applications. Inadvertent entrance of both fibrin and cyanoacrylate may risk thrombus (blood clot) formation (Ang, Tan, Tan, Ng, & Song, 2001; LeMaire et al., 2005; Middleton, Matthews, & Chiasson, 1991). Although cyanoacrylate-based adhesives have strong adhesive properties, they have been associated with aneurysmal dilatation (Carton et al., 1961) and tissue necrosis (Takenaka, Esato, Ohara, & Zempo, 1992). Recently developed adhesives have had promising results in repairing of high-pressure cardiovascular defects. One of the most promising adhesives is a hydrophobic light activated adhesive that demonstrated capability of closing 3 to 4 mm carotid artery defects and 2 mm full-thickness defects of the left ventricle in combination with a patch (Lang et al., 2014). Although this adhesive has shown comparable adhesive strength with cyanoacrylate adhesives, without the toxic effects, long-term studies are required for clinical approval.

A separate strategy that has been employed for replacing sutured anastomoses is a hybrid approach combining surgical adhesives with a mechanical coupling. Buijsrogge et al. reported a technique for end-to-side anastomosis using a extraluminal stainless steel frame with 4 downward facing hooks (Figure 12) (Buijsrogge et al., 2002). The device is inserted into the target vessel by inserting each hook element, then octyl-cyanoacrylate

adhesive is applied to consolidate the connection. Limitations of the device include a critical incision length, high external ring frame that can lead to kinking, and the adhesive used is only approved for external use (P. Tozzi, 2007). Other hybrid approaches have combined cuff systems with an adhesive, but all reports were limited to small vessels or low-pressure venous applications (Galvao, Bacchella, & Machado, 2007; Sacak, Tosun, Egemen, Sakiz, & Ugurlu, 2015).

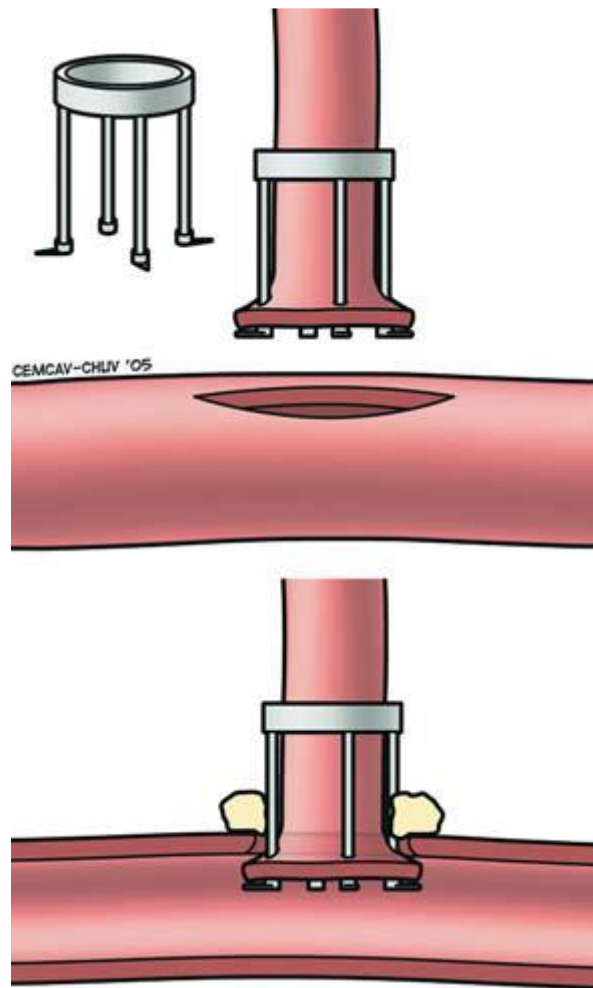


Figure 12: Drawing showing a hybrid mechanical and adhesive anastomosis device. Stainless steel ring has 4 hooks extended axially with thickening at the end that are elastic and can be bent for insertion. Vessel connection is consolidated by cyanoacrylate adhesive (P. Tozzi, 2007).

F. Device Design for LVAD Outflow Graft Anastomosis Device (GrAD)

The standard running suture technique is the preferred method for LVAD outflow graft anastomosis. However, this technique may be time-consuming, difficult to perform in constrained surgical spaces, and requires clamping of the aorta. Further, the progression of LVAD implantation surgery toward less-invasive and off-pump procedures increases the technical difficulty of completing standard hand-sewn LVAD outflow graft anastomosis due to uncompensated aortic flow dynamics and smaller surgical spaces. These limitations of the standard sutured anastomosis motivates the development of a novel method for sutureless LVAD outflow graft anastomosis.

1. Design Requirements for a LVAD Outflow GrAD

Table 1: Physiologic and mechanical design requirements for an LVAD outflow graft anastomosis device (GrAD).

Physiologic Design Requirements	Mechanical Design Requirements
Minimal foreign-body non-intimal surface area	Adaptable to range of graft diameters
Minimal tissue trauma	Adaptable to range of wall thicknesses
Minimal alteration of native tissue compliance	Attachable/detachable
Smooth profiles complementing intimal wall	Easily deformable and elastic
Angled conformation	Easily deployable in small spaces
Clampless	Recovery mode for device failure
	Economical

The general design criteria for an LVAD outflow graft anastomosis device (GrAD) are listed in Table 1. Any foreign material in the blood stream will likely trigger an inflammatory response (Anderson, Rodriguez, & Chang, 2008) and increase vessel wall stress (Scheltes, Heikens, Pistecky, van Aniel, & Borst, 2000). Additionally, foreign materials elicit intimal hyperplasia leading to gradual decrease of effective luminal area

for blood to flow. Tissue trauma, which may be caused by suture or pin vessel wall penetration, is another source contributing to triggering an inflammatory response and intimal hyperplasia (Kornowski et al., 1998). In principle, a device with zero foreign-body non-intimal surface exposure and tissue trauma is desirable to minimize inflammatory response, increase in wall stress, and intimal hyperplasia.

Minimal alteration of the native compliance at the anastomosis, smooth profiles of the device to the intimal wall, and angled conformation minimize the negative effects of the device on vessel wall and blood flow properties. Sutured anastomoses are often associated with changes in vessel compliance observed through increased wall rigidity and alteration of elastic modulus at the anastomotic site (N. Baumgartner, Dobrin, Morasch, Dong, & Mrkvicka, 1996). There may also be a reduction in luminal area observed at the sutured anastomoses, which has been shown to reduce further during systole (Figure 13) or as blood pressure increases (Tozzi et al., 2000a, 2000b). Abrupt profiles of devices to the intimal wall may disrupt the natural wall shear stress patterns, which is associated with thrombus formation and intimal hyperplasia (Fillinger et al., 1990; Ojha, 1994). Studies have demonstrated that anastomosis angle affects blood flow. The ideal anastomosis angle should be 30° to 45° (P. Tozzi, 2007). Anastomosis angles $> 60^{\circ}$ demonstrate reductions in expected flow and creation of blood stagnancy areas (Leva & Engström, 2003; Zhang, Moskovitz, Piscatelli, Longaker, & Siebert, 1995). Therefore, highly compliant, smooth profiled, and angled anastomosis may reduce the disposition for the development of myointimal hyperplasia and thrombus formation, as well as minimize the alteration of native vessel and blood flow properties at the anastomosis.

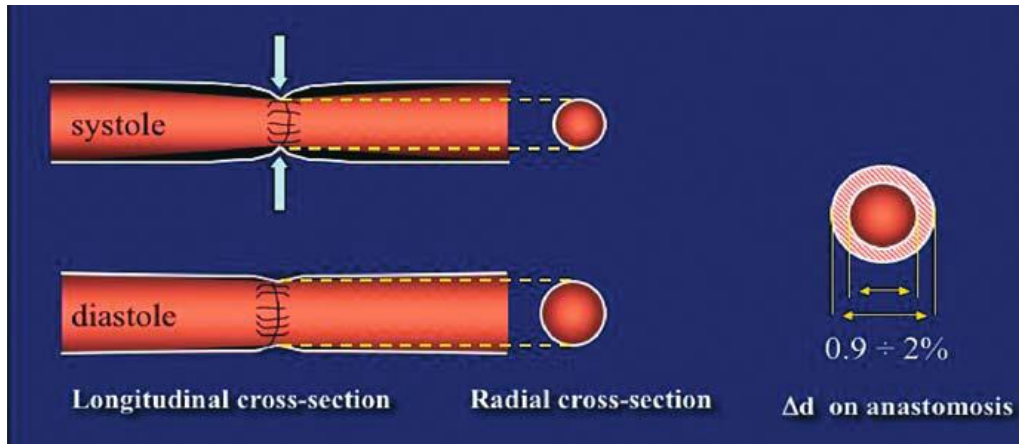


Figure 13: Diagram showing systolic movement of vessel edges at the anastomosis due to sutured anastomosis. Schematic shows the reduction in cross-section lumen at systole or higher pressure (P. Tozzi, 2007).

Clamping of the aorta creates an area of blood stagnancy such that an aortotomy can be created without the risk of hemorrhage (major loss of blood). Aortic clamping increases the risk of neurological complications (Zamvar et al., 2002) and aortic dissections (Stanger et al., 2002). For CABG procedures, clampless and off-pump procedures demonstrated lower mortality and stroke rates (Borgermann et al., 2012). A device allowing clampless anastomosis could similarly reduce the risk for any neurologic or aortic complications due to LVAD outflow graft anastomosis.

An LVAD outflow GrAD should be adaptable to a wide range of graft diameters and aortic wall thicknesses. LVAD outflow graft diameter range from 10 mm to 20 mm, varying between LVAD types. Aortic wall thicknesses may range from 2 mm to 4 mm based on sex, race, and age shown in Table 2. Wall thickness variability arises with elderly HF patients with calcified aortas that is shown to be associated with aortic wall thicknesses > 4 mm (Jang et al., 2012). To allow anastomosis of all LVAD outflow grafts to any patient, the GrAD should accommodate all graft diameters and adapt to any aortic wall thicknesses. LVAD outflow graft lengths are tapered to each patient by positioning the graft in its desired location and cutting off any unnecessary length in order to reduce

the risk for graft kinking due to superfluous graft length in the constrained thoracic cavity. Some LVAD systems require the inflow end of the graft to be secured prior to completion of the outflow anastomosis, limiting the surgeon to a single free-end of graft. An attachable anastomosis system would allow surgeons to appropriately size grafts to patients then attach the anastomosis system to the free-end. An easily deformable and elastic device are important characteristics for development of an efficient deployment mechanism for the device, allowing it to remain undamaged when collapsed into a deployment catheter or sheath. An easy deployment mechanism is especially critical in less-invasive procedures where surgical windows are confined. A method for safe recovery of the anastomosis in the case of device failure is also of critical importance since failure of an anastomosis may lead to catastrophic hemorrhage and potential death.

Table 2: Average and maximum wall thicknesses of ascending aorta. Large variability in wall thicknesses is shown based on sex, race, and age (Li et al., 2004).

Patient Demographics	No. of Subjects	Average Wall Thickness (mm)		Maximal Wall Thickness (mm)	
		Mean (SE)	<i>p</i>	Mean (SE)	<i>p</i>
Sex			0.028		0.010
Men	98	2.32 (0.06)		3.85 (0.13)	
Women	98	2.11 (0.06)		3.31 (0.13)	
Race			0.061		0.023
Black	99	2.15 (0.05)		3.74 (0.10)	
White	97	2.27 (0.05)		3.42 (0.10)	
Age range (yr)			< 0.001		0.002
45–54	66	2.03 (0.05)		3.33 (0.12)	
55–64	52	2.18 (0.06)		3.61 (0.13)	
65–74	39	2.26 (0.07)		3.56 (0.15)	
74–84	39	2.51 (0.07)		3.98 (0.16)	

2. Design Considerations for LVAD Outflow GrAD

There are three main design considerations for the development of a LVAD outflow GrAD:

- 1) Graft-to-vessel connection
- 2) Materials
- 3) Anastomosis biomechanical properties

3. Graft-to-Vessel Connection

There are four main mechanisms for connecting a sutureless device with either a graft or vessel: Pins, wall eversion, wall compression, and adhesion. Pins penetrate through the wall from either the inner lumen to the outside or from the opposite direction. If the pins push from the inside to the outside it allows the device to push outward radially reducing the risk of hemorrhage and generation of a dissection. If pins push from the outside to the inside the opposite occurs and there is an increased risk for hemorrhage and generation of dissection.

Wall eversion is restricted to the tubular member with a free-end and typically employs an anvil to achieve eversion. This technique has larger implications for vessel-to-vessel anastomosis, because it permits intima-to-intima contact. However, the main limitation of wall eversion is potential damage to the tissue itself as it is being everted, which is not a factor since the tubular member with a free-end being anastomosed would be a synthetic graft.

Wall compression is the most non-traumatic for the vessel wall if the two surfaces creating the compression are designed to allow for nutrient perfusion to the vessel wall itself. The advantage of this approach is it can easily be attached and detached. The limitation of this connection type is that it provides limited strength that can be catastrophic if it were to disconnect. Design limitations of previous devices relying on wall compression for connection include the amount of foreign material exposed inside of the vessel lumen. Coronary stents have demonstrated that large amounts of foreign material inside of vessel lumens results in intimal hyperplasia and re-stenosis (Lal et al., 2003). Another design limitation of previous wall compression devices is the strict design constraints for wall-thickness due to a single-body component participating in the compression.

Adhesive connection for anastomotic applications has been discussed earlier. Adhesives offer the advantage of minimal foreign-body exposure to the inner lumen. The main limitation of current hemostatic adhesives is that they have inadequate adhesive strength to connect tubular members alone or have toxic and/or thrombogenic properties in vascular applications.

4. Materials

Critical to any material implanted in the human body is that the material can interface with tissues without causing unacceptable harm to the body. Second, the material must have necessary material properties to accomplish and sustain their function for its intended implantation duration. For LVAD outflow graft anastomosis, materials must be capable of sustaining attachment to the continuously moving aorta for up to 8

years--the longest duration a LVAD has been implanted. Further, materials may contact blood flow exposing them to turbulent pressure and flow. Therefore, a LVAD outflow GrAD must ensure attachment in a dynamic environment to enable LVAD flow to the aorta, while having minimal impact on the major role of the aorta to dampen pulse pressures and provide blood to the body.

Materials that have been used for cardiovascular applications include shape-memory alloys and polymer textiles. Nitinol is one of the most commonly used metals for fabrication of sutureless anastomosis devices in the form of connectors, anvils, and self-closing sutures. Alternative metals that are also commonly used are stainless steel and cobalt-chromium alloy. These metals allow for fabrication of devices that can be collapsed into deployment tools for introduction through limited surgical spaces and deployment into their desired location. With limited blood exposure area, these bare-metals have served well as anastomosis connectors. Intimal hyperplasia is the main cause of long-term failure associated with metallic devices as tissue proliferation leads to narrowing and obstruction. Trauma to the nearby tissue from metallic devices leading to intimal hyperplasia is due to physical irritation rather than chemically induced from corrosion of the metal (Williams, 2008), suggesting that these metals have adequate corrosion resistance. When using shape-memory alloys, designs should minimize the surface area of the material exposed to blood and potential for vessel trauma (e.g. vessel penetration, friction rubbing) to reduce the extent of intimal hyperplasia.

Expanded polytetrafluoroethylene (ePTFE) and polyethylene terephthalate (PET, Dacron) compose the majority of polymers used for fabrication of vascular grafts and sewing rings. These polymers react similarly within the human body (Mueller &

Dasbach, 1994). Upon implantation, thrombus is formed within the pores and cellular infiltration occurs. Then cellular proliferation via fibroblasts provides tissue in-growth with connective tissue. For inner lumen surfaces of vascular grafts, intimal hyperplasia leads to deposition of cell layers lining the inner surface of the graft. Synthetic grafts are recognized to function reasonably in large diameter and high flow applications, where narrowing due to intimal hyperplasia has a smaller impact on overall flow and rarely leads to obstruction. The few reported cases of LVAD outflow graft obstruction were due to factors extrinsic to the graft (Bergmann, Kottenberg-Assenmacher, & Peters, 2007; Frogel, Vodur, & Horak, 2008; Kaplon et al., 2001; Weitzel, Puskas, Cleveland, Levi, & Seres, 2009). There are reports of synthetic graft degradation after 15 years of implant (Shiyya, Kunihara, Matsuzaki, & Sugiki, 2006; Van Damme, Deprez, Creemers, & Limet, 2005), however, the duration for graft degradation far exceeds that of current LVAD implantation durations. Therefore, ePTFE and PET should be acceptable graft materials for fabrication of a GrAD.

5. Biomechanical Properties

The natural biologic properties of vessels are altered by anastomosis, such as vessel compliance. Generally, more compliant anastomosis devices impart less influence on the natural elastic properties of the vessel which may reduce changes in wall stress and risk for intimal hyperplasia. It can be speculated that sutureless anastomosis devices fabricated from shape-memory alloys and elastic polymers will be more compliant than running suture anastomosis since these materials are more elastic than polypropylene suture. Alterations in blood flow is another concern as anastomosis angle and material

profiles in the blood stream may affect the flow patterns and wall shear stress at the anastomosis. Therefore, a highly compliant and 30° to 45° angle anastomosis, and smooth profiles of foreign bodies conforming to the luminal vessel wall may reduce potential risk of complications inherent to alterations of biomechanical properties of the native aorta. Patched or cuffed anastomoses have demonstrated better patency (Brumby, Petrucco, Walsh, & Bond, 1992) and lower peak wall shear stress (Harris, 1999; Walsh, Kavanagh, O'Brien, Grace, & McGloughlin, 2003). Subsequently, a sutureless LVAD outflow GrAD should promote the native biomechanical properties of the blood vessels and natural blood flow.

II. METHODS

A. Study Design

The objective of this study was to develop a LVAD outflow GrAD to facilitate anastomosis to the ascending aorta. To demonstrate proof-of-concept, the following aims were proposed:

- 1) Complete fabrication of a device enabling sutureless anastomosis of LVAD outflow graft to the ascending aorta
- 2) Complete feasibility testing of candidate prototype GrAD to demonstrate secure connection under static and dynamic pressures
- 3) Complete feasibility testing of candidate prototype GrAD to demonstrate comparable attachment strength as standard sutured anastomosis technique

Pressure Tests (n=3)			
Static Pressure Test Conditions	Dynamic Pressure Test Conditions	Data	
0, 50, 100, 150, 200 mmHg	Normal, Hypertension, Heart Failure, Partial VAD Support	Leak Rate	Leak Classification

Pull-out Tests (n=3)			
Test Conditions		Data	
Anastomotic Device	Sutured Anastomosis	Peak Pull-out Force	Failure Mode

Figure 14: Diagram showing experimental design consisting of static and dynamic pressure, and pull-out tests.

To successfully complete the proposed aims, three studies were completed: 1) static pressure testing (n=3), 2) dynamic mock loop pressure testing (n=3), and 3) paired pull-out force testing to compare GrAD to sutured anastomosis (n=3) (Figure 14).

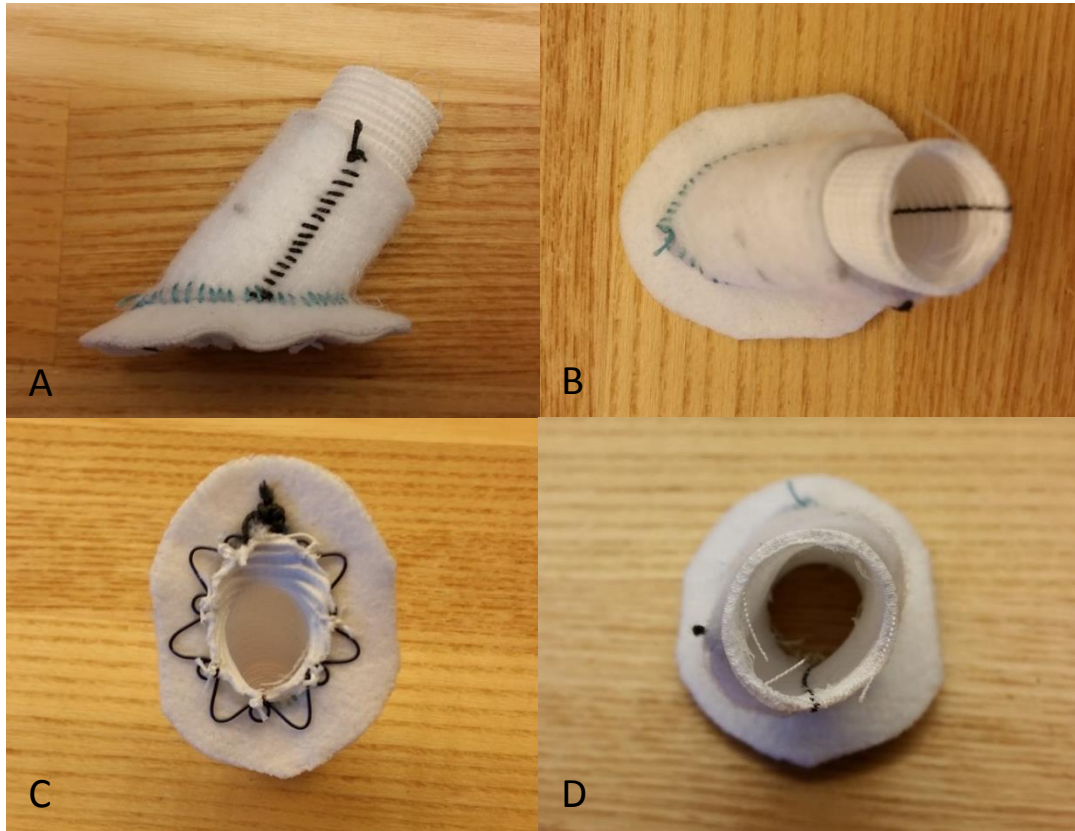


Figure 15: Photographs of various views of the prototype LVAD outflow graft anastomosis device (GrAD) consisting of a nitinol connector fastened to a 15 mm vascular graft and felt flanged cuff: A) Side-view, B) Top-view, C) Bottom-view, D) Top-view inside lumen of graft

The prototype GrAD comprised of an attachable nitinol connector, polymer felt flanged cuff, and adhesive (Figure 15). Prototypes of the components were fabricated and tested experimentally to investigate smooth conformation in plastic models and bovine aorta specimens. Preliminary testing of several adhesives was completed to assess capability of adhering the device to aortic tissue while maintaining connection without significant fluid leakage. The anastomosis device was tested in static pressure and dynamic mock loop pressure models using harvested bovine descending aorta and de-ionized (DI) water. Paired mechanical pull-out experiments for device completed

anastomosis and hand-sewn suture anastomosis attached to bovine descending aorta were performed to quantify peak tensile force measured in Newtons (N) before failure.

B. Prototype Design Development

Literature, patent application, and patent reviews were conducted to evaluate intellectual property of other potential competing devices developed for sutureless and end-to-side anastomosis. Based on the literature and patent review, and design considerations for a sutureless LVAD outflow GrAD, design specifications were established, as shown in Table 1. The design of combining a nitinol connector, polymer felt flanged cuff, and adhesive was selected for further development. Curvature of the CADs were dimensioned based on human adult ascending aorta dimensions (Rylski, Desjardins, Moser, Bavaria, & Milewski, 2014).

C. Nitinol Connector Fabrication

In order to fabricate each nitinol connector, metal frames were used to mount the wire into its desired shape, annealed in a high-temperature oven, and quenched in a cold-water bath. Flat and curved nitinol connectors were fabricated using several different gauges of nitinol wire. The various nitinol connector types were assessed for strength and fit using plastic model of an aorta (section of Zygon tubing) and bovine descending aorta (Figure 16).

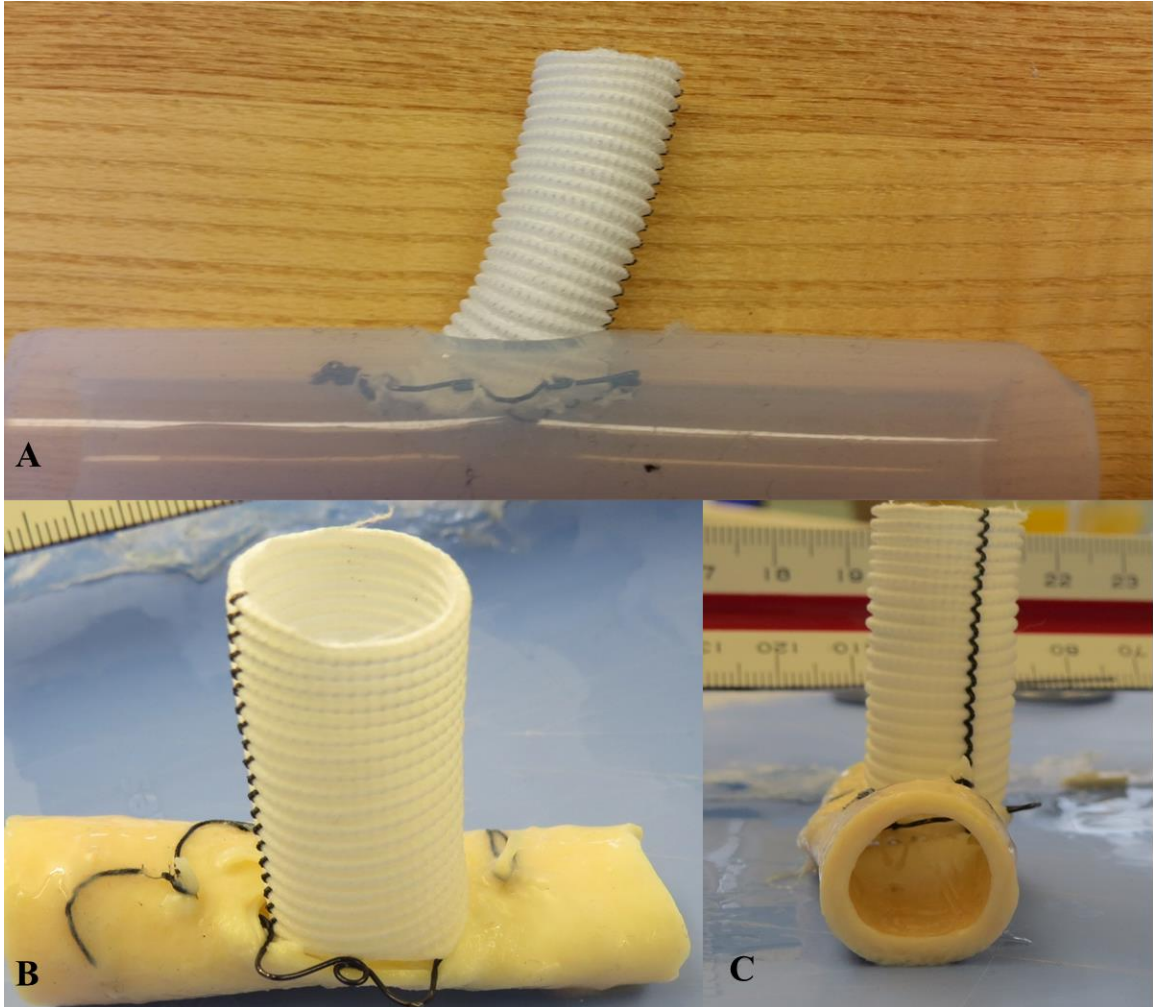


Figure 16: Photographs of preliminary fit studies of the nitinol connector within silicone tubing and bovine descending aorta specimens. A) Curved nitinol connector within silicone tubing showing curvature due to forces exerted by the tubing, B) Struts of a flat nitinol connector protruding out of the aorta due to rigidity of thick wire gages, C) Poor conformation of a flat nitinol connector to the inner lumen aortic wall that have the potential for causing complications

1. Frame Construction



Figure 17: Photographs of the nitinol connector frame fabrication. A) Mill used for boring holes according to template mounted onto copper slip coupling, B) Copper slip coupling used to create curved nitinol connectors, C) Steel plate used to create flat nitinol connectors.

For flat nitinol connector frames, 3.175 mm thick flat stainless steel plates were cut into 31.175 mm x 31.175 mm squares. For curved nitinol connector frames, 31.75 mm outer diameter copper slip couplings were used. Template drawings directing placement of screws for molding the nitinol shape were created using SOLIDWORKS 2015 and attached to the frames. With a mill, 2.0 mm titanium drill bit was used to bore holes for setting main shape of the connector and a 2.4 mm titanium drill bit was used for

anchoring the nitinol wire. Each hole was threaded using a 2-56 and 4-40 tap and die set for the 2.0 and 2.4 mm bored holes, respectively. Stainless steel screws corresponding to the threaded hole size were inserted into the frames. Photos of the completed frames are shown in Figure 17.

2. Shape Setting Nitinol

Super elastic temper, light oxide nitinol round wire (0.76, 0.50, 0.40, 0.36, 0.23, and 0.18 mm gauge) was used to create the nitinol connectors. The end of the nitinol wire was secured to the frames using binder clips and reinforced by wrapping the wire several times around the 4-40 anchoring screws. Then the wire was wrapped tightly around each of the 2-56 screws to form the desired shape and each screw was tightened to ensure that the wire was held securely in tension. The free-end of the wire was anchored by wrapping the wire around the anchoring screw. Excess wire was removed and the remaining end was secured to the frame with a second binder clip.



Figure 18: Photograph of candidate prototype nitinol connectors of various wire gauges, curved/flat members, and with/without loops.

Nitinol frames were placed in a Thermolyne Benchtop Muffle Furnace (ThermoScientific, Waltham, MA) pre-heated to 530°C for 9 minutes. Frames were removed from the furnace and quenched immediately in a room temperature bath of DI

water. After cooling, the frames were air-dried. Each screw was loosened and the wire was carefully removed from the frames. Excess wire was removed and the loose ends were fastened together using 2-0 Black Braided silk suture (Ethicon, Somerville, NJ). Figure 18 shows various candidate nitinol connectors that were assessed for fitting.

A single end of a 15 mm Gelweave Gelatin Impregnated Woven Vascular Prosthesis vascular graft (Vascutek Ltd, Glasgow, UK) was cut at a 45° angle. Each nitinol connector was fastened to the graft with 7 radially tied 2-0 Ethibond Excel polyester suture (Ethicon, Somerville, NJ). Combined graft and nitinol connector were inserted into 19.05 mm inner diameter Zygon silicone tube (Saint-Gobain North America, Malvern, PA) through a 15.0 x 21.2 mm axes elliptical hole. Combined graft and connector were assessed for ease of insertion and smooth conformation to the inner lumen. Select nitinol connector designs were further assessed using bovine descending aorta specimens for identical assessment parameters. Based on these preliminary assessments, additional 0.36 mm gauge curved nitinol connectors were fabricated for further experimentation (Figure 19).



Figure 19: Photographs of 0.36 mm gauge nitinol connector providing smooth conformation to the luminal wall of a bovine descending aorta specimen.

D. Felt Flanged Cuff Fabrication

Medical-grade polymer felt was cut and hand-sewn using 2-0 Ethibond Excel polyester suture (Ethicon, Somerville, NJ) to construct the flanged cuff structure as shown in Figure 20. Three coats of GE Silicone II (General Electric, Fairfield, CT) were applied to the exterior of each cuff, allowing each coat to cure for at least 30 minutes before re-application. After application of the final coat, they were allowed to dry for 24 hours before initiating static and dynamic pressure testing.

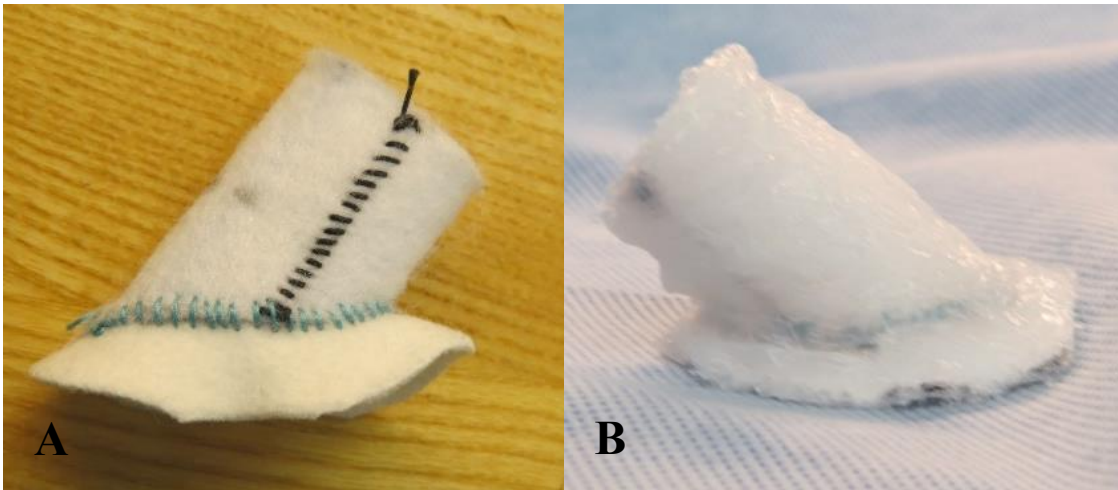


Figure 20: Photographs of prototype felt flanged cuff. A) Sewn flanged cuff without silicone coating, B) Flanged cuff with 3 coats of silicone.

E. Bovine Aorta Specimens

Descending aorta specimens were excised from adult male jersey calves within 6 hours of euthanasia. Specimens were removed carefully to maintain as much length of any branching arteries. Each vessel was immediately submerged in 3°C Belzer UW Cold Storage Solution (Bridge to Life Ltd., Columbia, SC) and cryopreserved at -80°C.

F. Static and Dynamic Pressure Testing

Cyanoacrylate, octylacrylate, and fibrin/thrombin adhesives were tested for adequate attachment strength of the GrAD to the bovine descending aorta specimens. The selected adhesive for attachment was cyanoacrylate. After thawing bovine descending aorta specimens, any branching arteries were tied off using 3-0 silk ties. If there was inadequate length to tie off branching arteries, 5-0 Prolene suture was used to cinch the hole shut and a drop of cyanoacrylate adhesive was applied for sealing. Tubing connectors were inserted into each end of the aorta specimen and secured using a combination of 2-0 silk ties and zip ties. Elliptical aortotomies were created in bovine descending aorta specimens (n=3) with major and minor mean axis \pm standard deviation lengths of 10.5 ± 0.4 mm and 15.7 ± 0.9 mm, respectively. Combined graft and nitinol connectors were inserted through the aortotomy. Using opposition by pulling the free-end of the graft, the flanged cuff was slid down the exterior of the graft to interface snug with the exterior of the aorta. .07 mL of cyanoacrylate adhesive was applied between the flanged cuff and vessel, and between the graft and flanged cuff. Each anastomosis was allowed to cure for 30 seconds before attaching the vessel to the static/dynamic mock loop in its natural forward flow orientation. A new nitinol connector and flanged cuff was used for each experimental set.

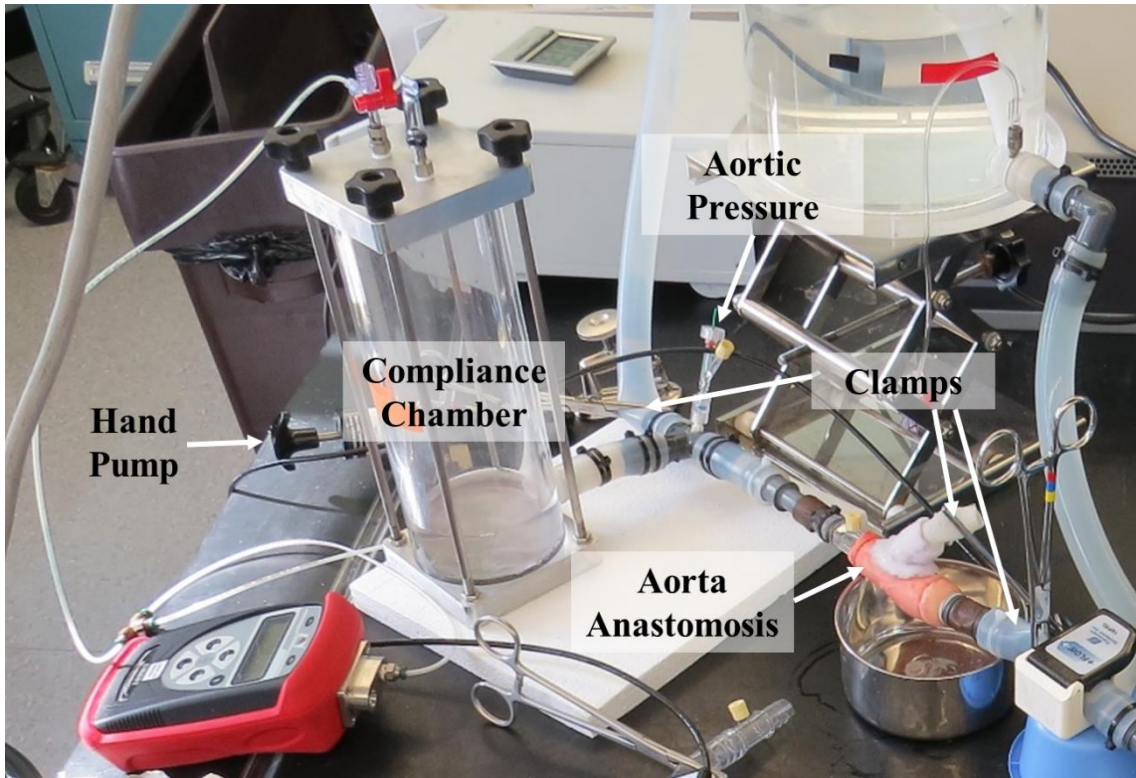


Figure 21: Photograph showing experimental setup for static pressure testing.

The experimental setup (mock loop model) used for static pressure testing is shown in Figure 21. For each vessel an internal pressure of 0, 50, 100, 150, and 200 mmHg was applied and maintained at steady-steady (± 2 mmHg) at each pressure step for 30 seconds, and any fluid leakage from the anastomosis was collected in a basin placed underneath the vessel. Total fluid loss at each pressure step was measured using a graduated cylinder. Fluid leak rate was calculated using the following equation and converted to mL/min for reporting:

$$\frac{\text{Volume of Total Fluid Loss (mL)}}{30s} * \frac{60s}{1min} = \frac{mL}{min} [\text{Leak Rate}]$$

Pressure was set using a pressure hand pump (Meriam Process Technologies, Cleveland, OH) connected to a SMART Manometer (Meriam Process Technologies, Cleveland, OH) and an air column compliance chamber via a three-way adapter. Internal

pressure was measured using a Mikro-tip Pressure Transducer (Millar, Houston, TX) and continuously monitored with Labchart 8 (AD Instruments, Sydney, Australia).

Table 3: Hemodynamic tuning parameters for each dynamic mock loop condition.

	Normal	Hypertension	Heart Failure	Partial Support
Art_{mean} (mmHg)	90 - 110	> 120	< 90	80 - 100
ArtP_{systolic} (mmHg)	110 - 130	> 140	< 100	100 - 120
ArtP_{diastolic} (mmHg)	70 - 90	> 100	< 60	60-90
AoF_{mean} (L/min)	4.5 - 5.0	4.5 - 5.0	3.0 - 4.0	4.0 - 5.0
VADF_{mean} (L/min)	0.0	0.0	0.0	2.0 - 3.0

Dynamic pressure testing was completed using the mock flow loop model shown in Figure 22. The simulated test conditions and hemodynamic parameter requirements of each condition are shown in Table 3. The following hemodynamic measurements were continuously recorded for 30 seconds at a 400 Hz sampling rate using Labchart 8:

1. Aortic Pressure (AoP) – mmHg
2. Arterial Pressure (ArtP) – mmHg
3. Aortic Flow (AoF) – L/min
4. Ventricular Assist Device Flow (VADF) – L/min

Fluid leakage from the anastomosis was collected during each data set and measured using a graduated cylinder. Mikro-tip Pressure Transducers were used to measure pressure and PXL Clamp-on Flowsensors (Transonic Systems Inc., Ithaca, NY) to measure flow. The mock ventricle was fitted with a single leaflet mechanical valve at the inlet and a trileaflet mechanical valve at the outlet with filling and ejection controlled using a customized pulse duplicator (LB Technology LLC, Louisville, KY). A Castaloy

clamp (Thermo Fisher Scientific, Waltham, MA) was used to vary afterload resistance. An air-filled column chamber was used to vary compliance. For the LVAD support test condition, a HeartMate II (Thoratec Corp., Pleasanton, CA) was used. All hemodynamic data were signal conditioned using a custom data acquisition system (Koenig et al., 2004). All pressure and flow transducers were pre- and post-calibrated using an established technique (Koenig et al., 2004).

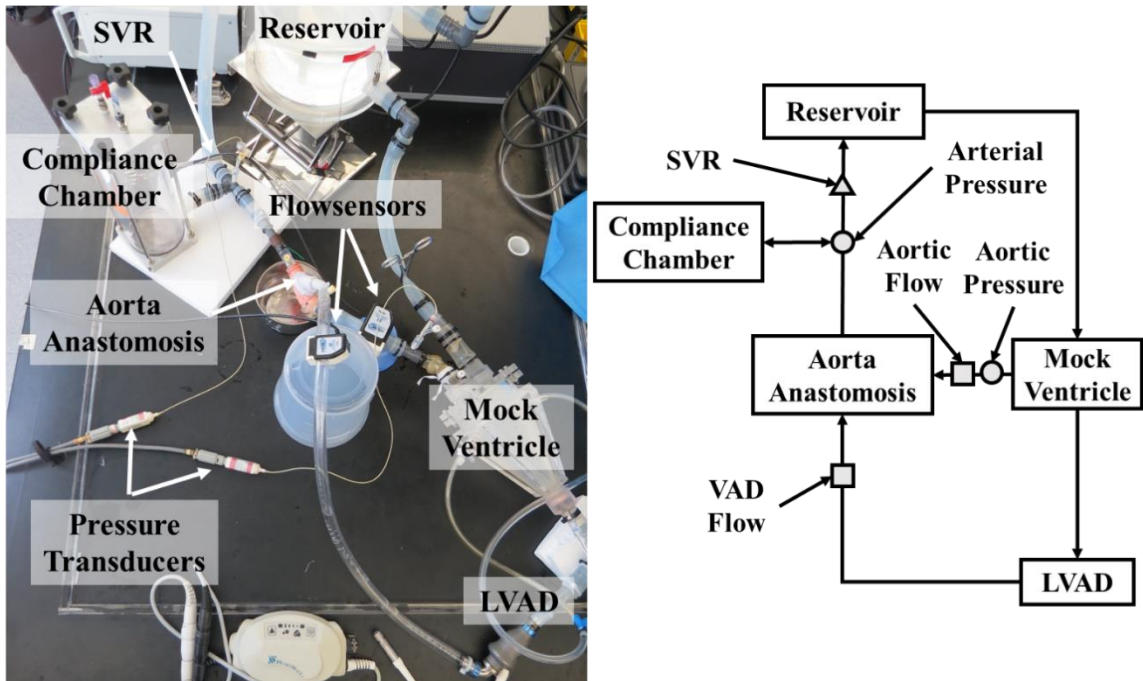


Figure 22: Photo and block diagram showing experimental setup for dynamic mock loop pressure tests; Systemic vascular resistance (SVR); left ventricular assist device (LVAD).

G. Pull-out Testing

The experimental setup for mechanical pull-out testing is shown in Figure 23. Following completion of the static and dynamic pressure tests, an experienced cardiac surgeon anastomosed a 15 mm GelWeave graft in a running suture technique with 4-0 Prolene suture onto the same aortic specimen used in static and dynamic pressure tests (note: same person performed all hand sutured anastomosis for all tests). For each vessel,

a hand-sewn anastomosis was constructed on the opposite side of the previously attached anastomosis device. A 12.7 mm diameter round bar was passed through the vessel, which was then mounted to a 609.6 x 609.6 x 12.5 mm piece of slate. The graft from the anastomosis being tested was secured in-between two metal plates with sandpaper adhered to the contacting surfaces. #16 wire was passed through a bored hole through the plates to attach the graft to a HF-50 Force Gauge (M&A Instruments Inc., Arcadia, CA). A preload of 2.5 ± 0.5 N was applied before hand-pulling the gauge vertically upwards until failure and peak force was achieved and recorded. Each vessel and graft was photographed at the original site of the anastomosis. The hand-sewn anastomosis or device anastomosis was randomly selected to be tested first, but it was ensured that at least one from each group was tested first.

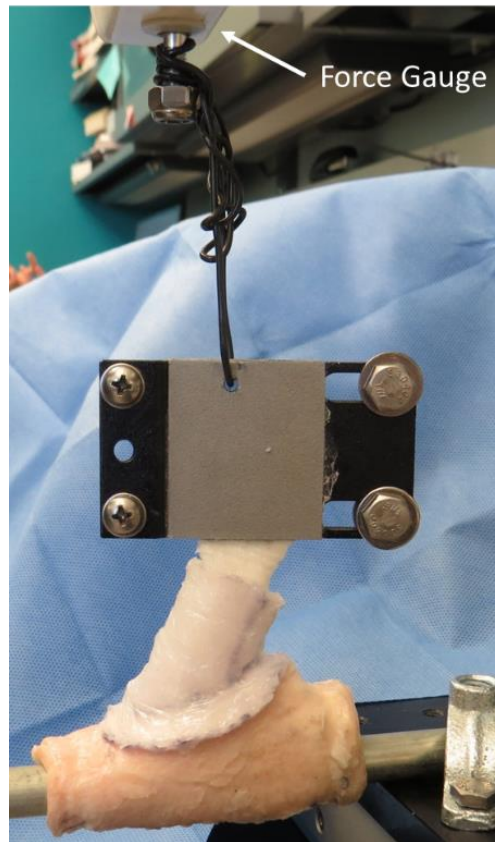


Figure 23: Experimental setup for pull-out testing.

H. Analysis Methods

The mean hemodynamic parameter values recorded during the dynamic pressure testing were calculated on a beat-to-beat basis using Labchart 8. Previously reported results for blood leakage rates under normal dynamic pressure (120/80 mmHg) associated with hand-sewn suture anastomoses (Sergeant, Kocharian, Patel, Pfefferkorn, & Matonick, 2016) were used for comparison. All statistical tests were performed using GraphPad Prism (GraphPad Software Inc., La Jolla, CA) and a 95% confidence level ($p < .05$) was used for determining statistical significance.

III. RESULTS

A. Final Prototype Design

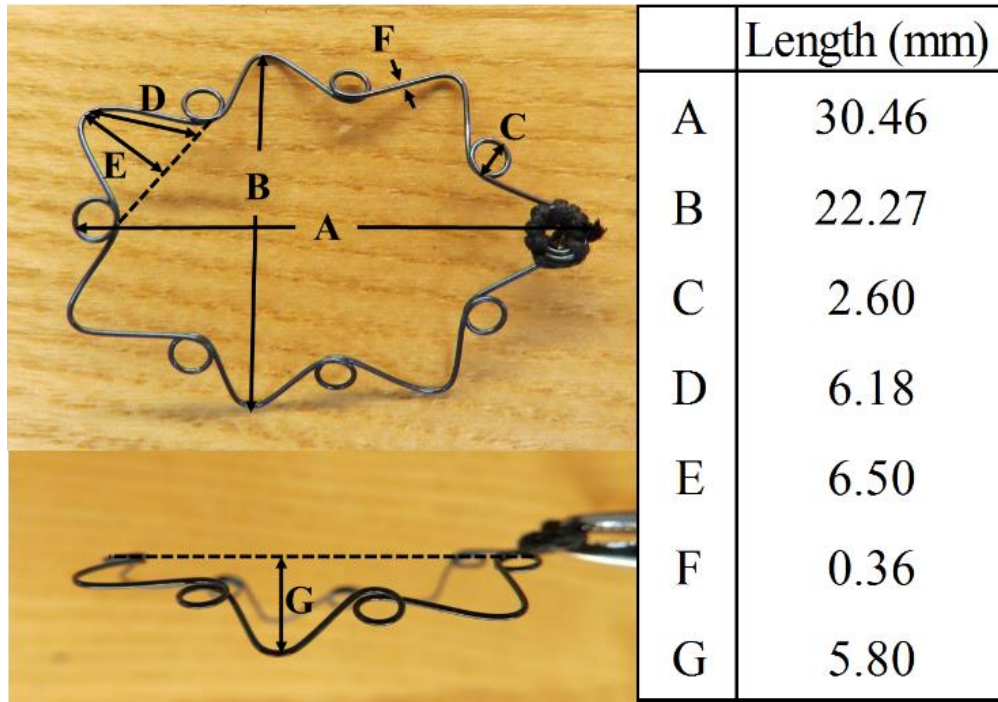


Figure 24: Dimensions of the prototype nitinol connector used for experimentation.

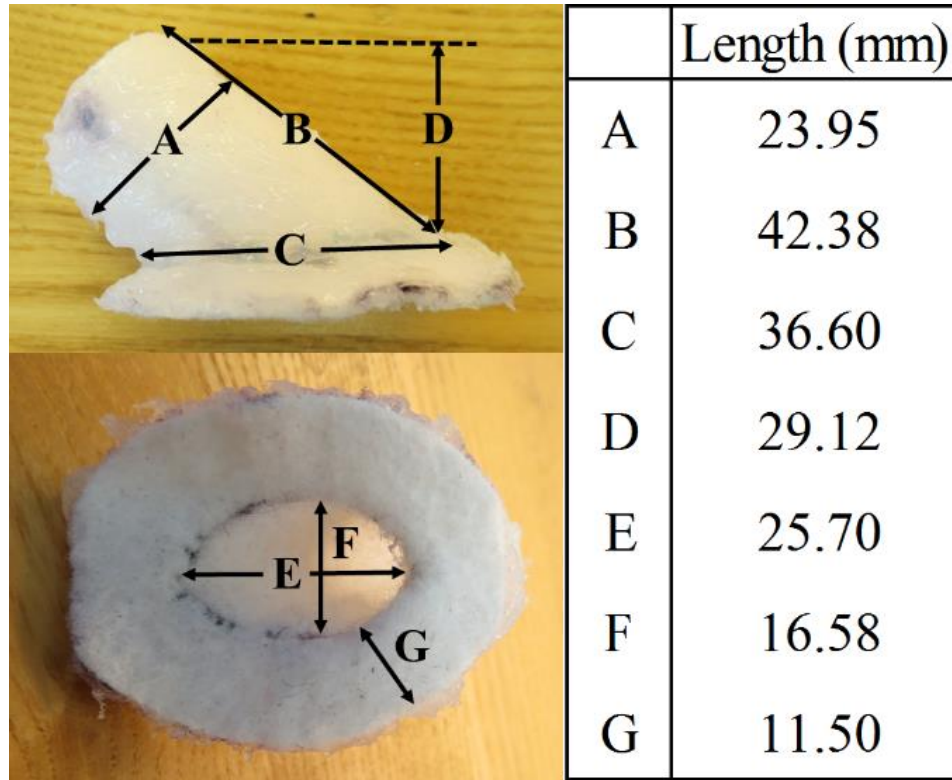


Figure 25: Dimensions of the prototype flanged cuff used for experimentation.

The dimensions for the nitinol connector and flanged cuff that were tested experimentally are shown in Figures 24-25. A curved 0.36 mm thick nitinol wire with intermittent spring elements was selected based on ease of collapsibility, smooth conformation to the luminal vessel wall, adequate rigidity to remain within the vessel, and capability to be fastened to a vascular graft. The addition of spring elements enhanced the collapsibility of the connector and provided a graft attachment point.

B. Static Pressure Testing

A summary of the leak rates for all static pressure steps are presented in Table 4. There was an increase in mean leak rate with increasing pressure for all device completed

anastomoses. All leaks were categorized as drips. Notably, a consistently larger leak rate was reported in vessel #2 at all pressure steps (Figure 26).

Table 4: Mean \pm standard deviation of leak rates from static pressure tests.

Pressure (mmHg)	Leak Rate (mL/min)
0	0.00 \pm 0.00
50	5.6 \pm 7.1
100	11.9 \pm 11.4
150	22.7 \pm 20.7
200	43.6 \pm 23.4

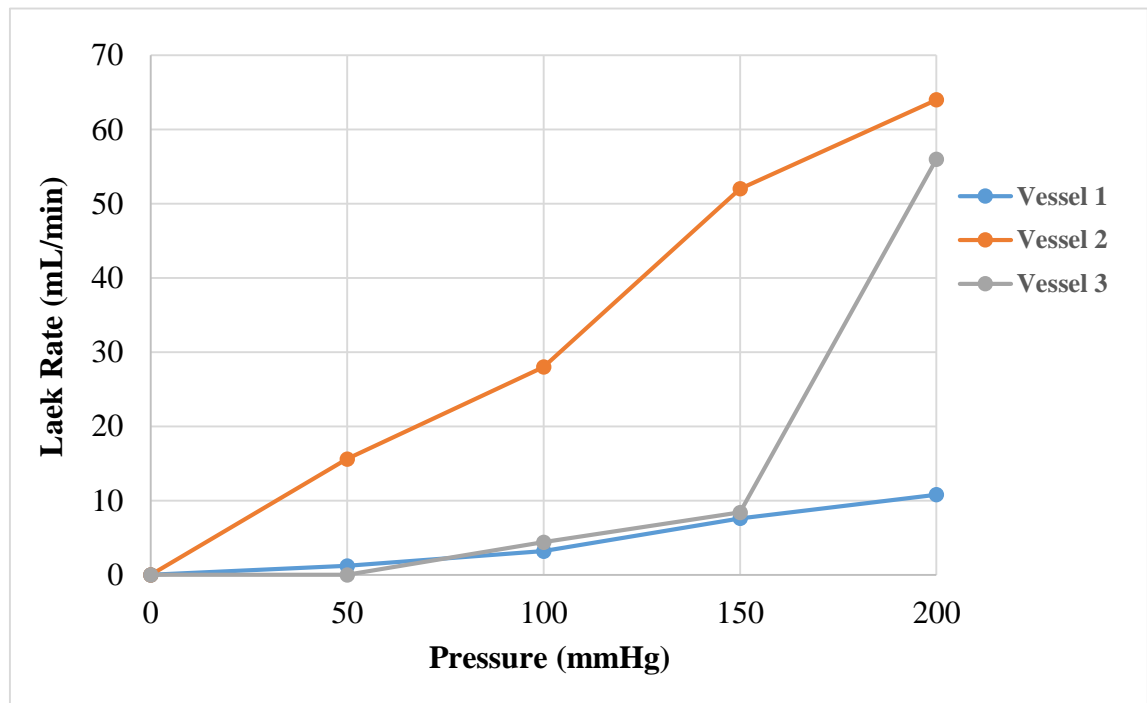


Figure 26: Leak rates for each vessel during static pressure tests. Vessel 2 consistently showed greater leak rates at all pressures \geq 50 mmHg.

C. Dynamic Pressure Testing

Each of the dynamic pressure test conditions met the aforementioned hemodynamic requirements for ArtP, AoF, and VADF. Pressure trends consistent with other mock loop studies (Bartoli et al., 2010; Giridharan et al., 2015) were observed in ArtPmean, PAoPmean, AoF, and VADF between conditions (Table 5, Figure 27):

- 1) Increased mean pressures from normal to hypertension
- 2) Decreased mean pressures and AoF from normal to heart failure
- 3) Increased mean pressures and flows from heart failure to LVAD support

Sample pressure and flow waveforms for each dynamic pressure test condition are shown in Figure 28.

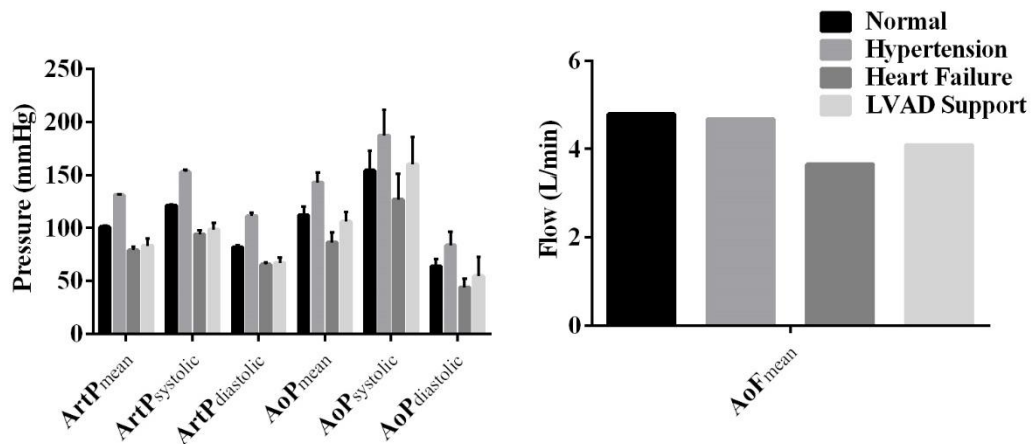


Figure 27- Graphs comparing pressure and flows for each dynamic mock loop condition reflecting typical physiologic trends in hemodynamic parameters associated with each condition; arterial pressure (ArtP); aortic pressure (AoP); aortic flow (AoF); left ventricular assist device (LVAD).

Table 5: Mean \pm standard deviations of hemodynamic parameter measurements calculated on a beat-to-beat basis for dynamic mock loop tests; arterial pressure (ArtP); aortic pressure (AoP); aortic flow (AoF); ventricular assist device flow (VADF); left ventricular assist device (LVAD)

	Normal (n=3)	Hypertension (n=3)	Heart Failure (n=3)	LVAD Support (n=3)
ArtP_{mean} (mmHg)	100 \pm 2	131 \pm 1	79 \pm 4	83 \pm 7
ArtP_{systolic} (mmHg)	121 \pm 1	153 \pm 2	94 \pm 4	99 \pm 6
ArtP_{diastolic} (mmHg)	82 \pm 2	111 \pm 3	65 \pm 2	67 \pm 5
AoP_{mean} (mmHg)	112 \pm 8	143 \pm 10	86 \pm 10	106 \pm 9
AoP_{systolic} (mmHg)	154 \pm 18	187 \pm 24	127 \pm 24	160 \pm 26
AoP_{diastolic} (mmHg)	64 \pm 7	84 \pm 13	44 \pm 8	55 \pm 18
AoF_{mean} (L/min)	4.79 \pm 0.14	4.67 \pm 0.11	3.65 \pm 0.19	4.09 \pm 0.09
VADF_{mean} (L/min)	0.00 \pm 0.00	0.00 \pm 0.00	0.00 \pm 0.00	2.49 \pm 0.26

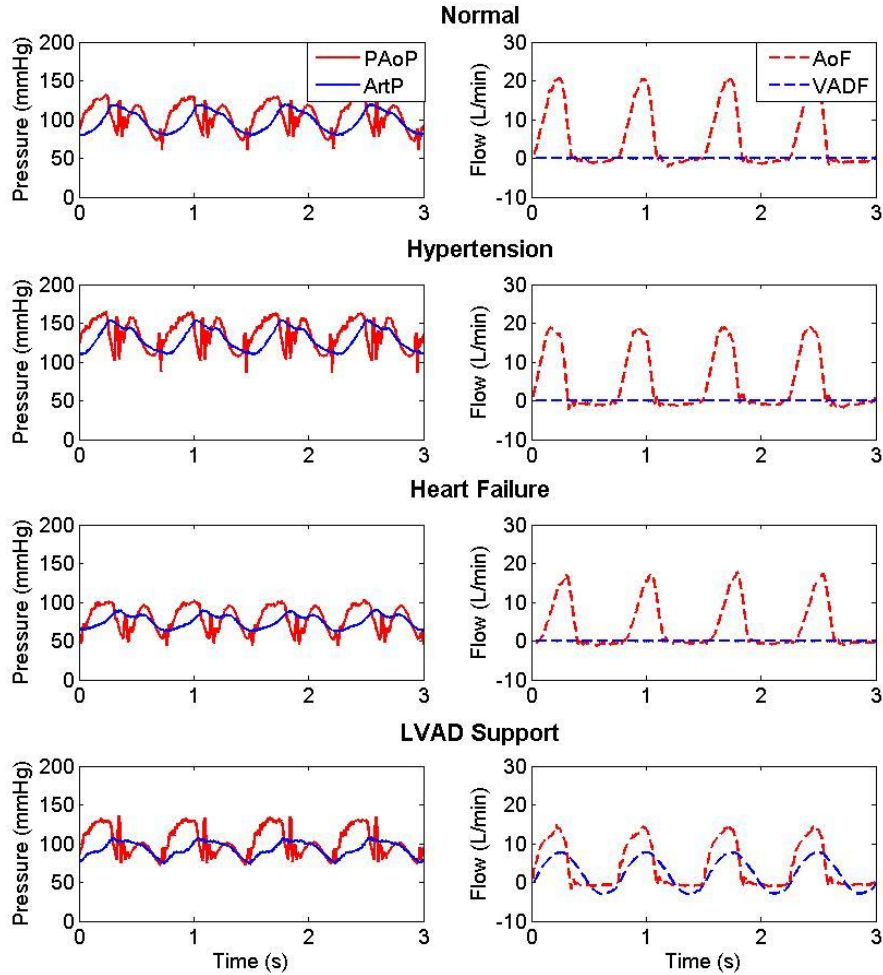


Figure 28: Sample waveforms collected for normal, hypertension, heart failure, and LVAD support dynamic mock loop tests.

The leak rates recorded for dynamic pressure tests are listed in Table 6, and the leak rates for the static and dynamic pressure tests are shown in Figure 29. Although a noticeable positive correlation was observed between mean leak rate and mean pressures, no statistically discernible differences were observed. The leak rates for normal mock flow loop condition and literature reported leak rates for sutured anastomosis are shown in Figure 30. A one-way ANOVA demonstrated a significant difference in leak rate between the GrAD and sutured anastomosis ($p \leq 0.05$) was observed. A Tukey comparison test showed significant differences in leak rates between the GrAD and Prolene 2, as well e-PTFE sutures (Table 7, Figure 30). No differences in leak rate between the GrAD and other sutures were statistically discernible. All leaks were categorized as drips.

Table 6: Mean \pm standard deviation leak rates for dynamic mock loop pressure tests; left ventricular assist device (LVAD)

Hemodynamic Condition	Leak Rate (mL/min) (n=3)
Normal	22.1 \pm 9.3
Hypertension	23.1 \pm 10.1
Heart Failure	16.4 \pm 6.4
LVAD Support	16.4 \pm 4.3

Table 7: Specifications for typical suture types used for anastomosis; needle:suture diameter ratio (N:S Ratio); polytetrafluoroethylene (PTFE).

	Suture Size	Needle Type	N:S Ratio	Suture Material
<i>Sergeant et al. Study Sutures</i>				
Hemo-Seal Prolene (HS)	5-0	C-1	1.84:1	Monofilament polypropylene
Prolene 1 (PR1)	5-0	C-1	2.41:1	Monofilament polypropylene
Prolene 2 (PR2)	5-0	C-1	2.06:1	Monofilament polypropylene
e-PTFE (PTFE)	CV-6	TTc-13	1.4:1	Monofilament e-PTFE
<i>Additional Graft Sutures</i>				
Prolene 3	3-0	SH	2.6:1	Monofilament polypropylene
Prolene 4	4-0	SH	3.47:1	Monofilament polypropylene
Prolene 5	5-0	SH	5.2:1	Monofilament polypropylene

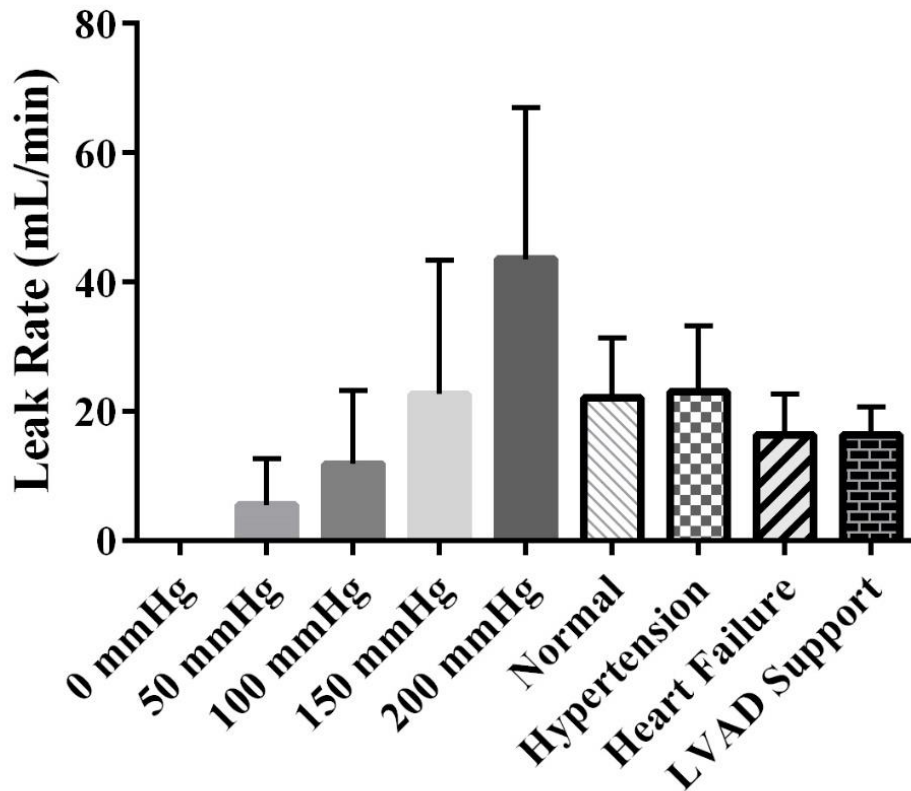


Figure 29: Leak rates for static and dynamic pressure tests; left ventricular assist device (LVAD).

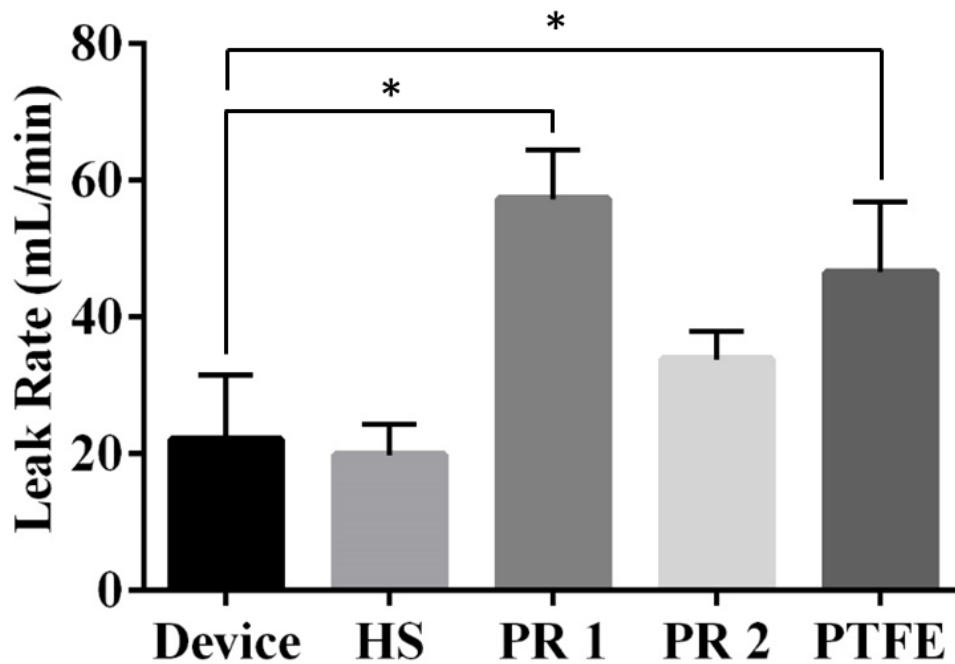


Figure 30: Graph comparing mean leak rate from graft anastomosis device (GrAD) and literature reported leak rate of Hemo-Seal (HS), Prolene (PR 1, PR 2), and expanded-polytetrafluoroethylene (PTFE) sutures. Asterisks show significant differences between GrAD and PR1 and PTFE ($p < .05$).

D. Pull-Out Testing

A comparison of peak pull-out forces for the GrAD and suture anastomosis is shown in Figure 31. The sutured anastomosis had a 19.9 N higher mean peak pull-out force than the device anastomosis, but paired t-test showed no significant difference in means.

Sample photos of the anastomosis device and aorta at the site of the anastomosis after pull-out testing are shown in Figure 32. All modes of failure for the GrAD appeared to be due to delamination of the adventitia (outermost layer of vessel tissue) based on the confluent layer of tissue observed on the flange face attached to the aorta. This was further supported by the discernably continuous difference in tissue color and depth on

the aorta at the site of the failed anastomoses. No signs of damage were observed in the nitinol connector or flanged cuff for all samples.

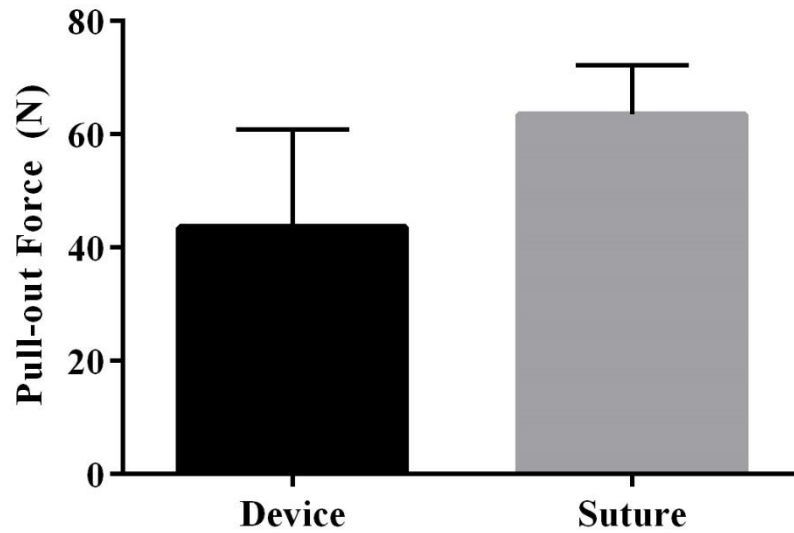


Figure 32: Peak pull-out force for graft anastomosis device (GrAD) and sutured anastomosis.

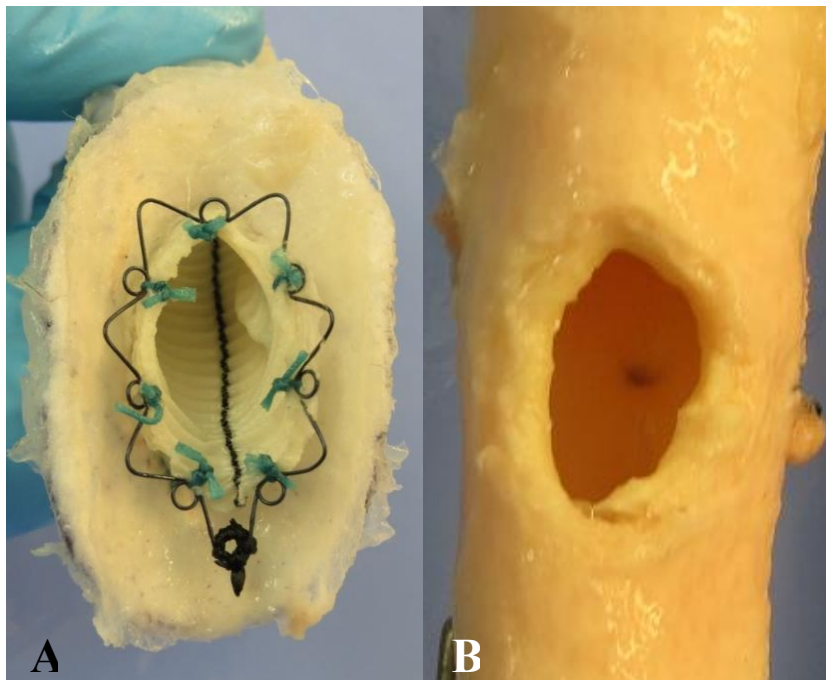


Figure 31: Photographs of the graft anastomosis device (GrAD) after pull-out testing with no indications of device damage. A) The debonded device with an observable layer of adventitial tissue on the flanged cuff, 2) Bovine descending aorta after delamination of a portion of the adventitial tissue by the device.

Sample photos of the suture and aorta at the site of the anastomosis are shown in Figure 33. The mode of failure for two of the suture anastomoses was due to the tissue tearing propagating from the suture holes. This was supported by the slits observed at every suture hole on the aorta and the remaining tissue within the intact sutures. For Vessel 2, the mode of failure appeared to be in part due to tissue tear propagation, as well as fracture of the suture. This was supported by the absence of slits propagating from a portion of the suture holes. Furthermore, a sliver of tissue remained where the suture was intact, but no tissue remnants were observed where the suture fractured (Figure 33).

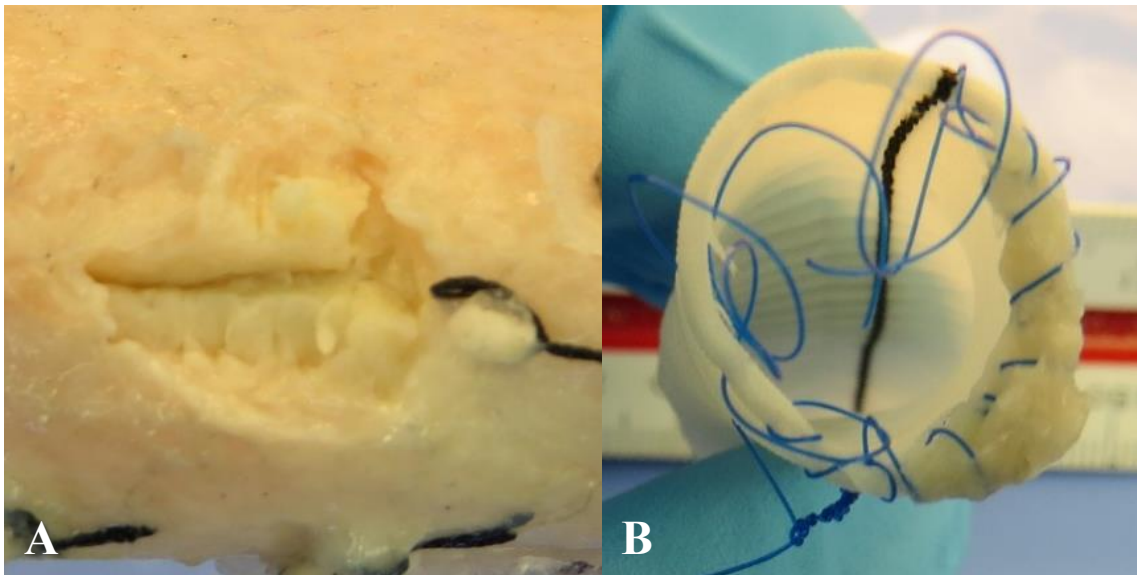


Figure 33: Photographs of the suture anastomosis after pull-out testing. A) Anastomosis site on the aorta where slits from suture ripping vessel can be observed, B) Fractured suture with a sliver of aortic tissue remaining.

IV. DISCUSSION

In regards to static pressure and dynamic pressure testing, all GrADs remained securely attached throughout all physiological hemodynamic test conditions. All leak rates were classified as drips that may have clotted if whole blood had been used (instead of water). The majority of leaks were observed to originate from the vascular graft that was uncovered by the flanged cuff and from ineffectively closed branching vessels from the aorta. Leaking innate to the device originated from the attachment of the graft and flanged cuff. It is speculated that a poor seal was created where the cuff, graft, and aortotomy interfaced. Alternative adhesives or solutions for attaching the flanged cuff and graft material may mitigate or effectively seal this connection point from leaking.

Comparison of leak rates under normal physiologic pressure (120/80 mmHg) between the GrAD and sutures showed statistically significant lower leak rate by the device compared to Prolene 1 and PTFE suture, and no statistically discernible differences were observed in comparing Hemo-Seal Prolene and Prolene 2 (Table 07). Sergeant et al. evaluated needle-hole blood leakage of various suture types from an end-to-end anastomosis of ePTFE grafts at normal physiologic pressures (120/80 mmHg) (Sergeant et al., 2016). Higher needle:suture (N:S) ratios were associated with higher leak rates; therefore, it can be speculated that leak rates of other common sutures for

anastomosis with larger N:S ratios (Prolene 3, Prolene 4, Prolene 5) may have resulted in significantly higher leak rates similar to Prolene 1. There were several differences in experimental design between the Seargent et al. study and the normal dynamic pressure test in this project, including: 1) an anticoagulated blood solution as opposed to DI water, 2) non-porous ePTFE grafts were used rather than gelatin-impregnated porous PET. Anticoagulated blood has been previously shown to leak from a syringe tip at rate 5.5 times slower than water (Elblbesy, 2014). The non-porous ePTFE graft did not contribute to the total leak rate, whereas leakage from the porous gelatin-impregnated grafts was included in the total leak rate in these experiments. The lower associated leak rate of blood and non-porous graft material would suggest that suture leak rates in the Seargent et al. study should be less than the device. These variations may have contributed, in part, to the 11.6% reduction in mean leak rate of Hemo-Seal suture compared to the device, although it was demonstrated that the GrAD produced similar leak rates as conventional sutures used for anastomosis.

In regards to peak pull-out strengths, no statistically significant differences were discerned between GrAD and sutured anastomosis. Based on the GrAD failure mode attributed to delamination of the adventitial layer of the aorta, pull-out strength is believed to be dependent on the strength of the bonds between aortic tissue layers suggesting that the bond strength provided by cyanoacrylate adhesive between the flanged cuff and aortic tissue is stronger than the bond strength between the layers of the aorta. Comparatively, pull-out strength for suture anastomosis is believed to be dependent on the strength of the suture and the strength of the aortic wall against an opening mode tearing fracture.

Sutureless connection to the aorta minimizes potential risk of tissue trauma inherent to the presence of non-absorbable sutures through the tissue. It may also reduce the time required to complete the anastomosis and be configured for a range of aortic thicknesses and graft diameters. Since this device employs a two component attachment method to compress the aortic wall, it is not limited by narrow range of aortic thickness specifications associated with the Symmetry and Pas-PORT devices. Up-scaling or down-scaling the connector dimensions to accommodate different graft diameters would simply require proportional scaling of the frames used to fabricate the rings. In GrAD design, an angled anastomosis is maintained by the flanged cuff which has been shown to promote superior blood flow dynamics and reduce the risk of clinical adverse events.

An important design consideration is the selection and/or development of a surgical adhesive. Acrylate-based adhesives, including cyanoacrylate, have not been approved for human internal use and have been reported to be toxic and thrombogenic. Fibrin glue adhesives, which are approved for human internal applications, were evaluated as a candidate adhesive for the device. However, we chose to use water (rather than whole blood) to demonstrate early feasibility, which did not allow clot formation and likely resulted in a higher leak rate. Fibrin sealant has been used to achieve hemostasis at the higher pressure levels in the arterial systems (B. Baumgartner, Draxler, & Lewis, 2016; N. Baumgartner et al., 1996; Detweiler, Detweiler, & Fenton, 1999), warranting further investigation of fibrin and other adhesives as an alternative solution. In this study, it was demonstrated that cyanoacrylate is capable of securely attaching LVAD

outflow grafts to the aorta, and is worth further consideration and investigation as a potential clinical sealant.

A. Limitations

To demonstrate proof-of-concept of device performance and early feasibility of device function, a small sample size (n=3) for each test was performed. Larger sample size based upon a power analysis will be required to demonstrate statistical significance, which will likely be performed once a design freeze has been achieved. A limitation associated with the static and dynamic leak testing was that in quantifying the leak rate, the fluid volume from the graft and branching vessels (not completely closed) were included in the overall leak rate calculation. For example, Vessel #2 was observed to be leaking in large part from the graft section that was not covered by the flanged cuff, which may be attributed to protein degradation of the gelatin that was impregnated into the porous graft. Vessels #1 and #3 were not observed to be leaking as profusely from the graft during static pressure tests. A second limitation of the pressure experiments was the use of water rather than whole blood, which represented a lower viscosity as is seen in anticoagulated blood and a worst case for leak rate. In future testing, the leak rate should be lower with the use of whole blood. A limitation associated with the pull-out tests was the apparatus constructed for testing. Since the force gauge was pulled vertically by hand, inconsistent directional tension may have been applied to each test sample. Second, the velocity that the force gauge was pulled may have varied for each test sample. These variables could be addressed if future pull-out experiments were conducted using a universal testing machine.

Cryopreservation methodology of the bovine descending aorta specimens may have altered the natural mechanical and molecular properties compared to fresh harvested tissue. UW solution is a commonly used solution hypothermic storage of blood vessels to minimize cellular degeneration (Abrahamse, Dinant, Pfaffendorf, & Van Gulik, 2002). However, hypothermia and cryopreservation has been shown to induce cellular damage (Wille, de Groot, & Rauen, 2008). Previous studies comparing vessel mechanics of fresh and cryopreserved tissues have reported contradictory results on the effects of cryopreservation, although a majority have found no significant differences (Stemper et al., 2007). A recent study demonstrated that vessels maintained physiological mechanics after 3 months of cryopreservation (Stemper et al., 2007). All bovine descending aorta specimens used for experiments were stored at -80°C for 3 to 4 months before experiments using similar established methods for cryopreservation. There is still a potential that the hypothermic storage, tissue handling, and series of experiments could have altered the behavior of the tissue affecting the results of this project. Fresh aortic segments may have reduced any variability due to tissue handling or storage.

V. CONCLUSION

The primary objective of this MEng thesis to develop a novel device that facilitates LVAD outflow graft anastomosis by demonstrating proof-of-concept and feasibility of prototype design. The preliminary data demonstrated feasibility as evidenced by secure connection to the aorta over a wide range of physiologic static and dynamic pressures, as well as leak rates and connection strength comparable to conventional hand-sutured anastomosis. Future developmental work should focus on (1) alternative adhesive exploration and (2) deployment tool. Since the nitinol connector and flanged cuff are collapsible, the components can be easily loaded into a deployment tool for device delivery. A dedicated deployment tool would also allow for the device to be deployed in small surgical windows using less invasive surgical techniques.

Three key characteristics of the prototype GrAD that may facilitate LVAD outflow graft anastomosis are: 1) sutureless connection to the aorta, 2) adaptable to various aortic thicknesses and graft diameters, and 3) 30-45° angled anastomosis. This novel device could provide an alternative method for LVAD outflow graft anastomosis that may be completed faster, more consistently, and with less dependence on surgical skill than conventional hand-suturing, thereby potentially allowing outflow anastomosis to be completed less-invasively. The device enables a sutureless, adaptable, and angled

anastomosis. Thereby, it has the potential of facilitating less-invasive LVAD implantation, faster implant time, and improving the reliability and reproducibility with the potential to improve patient outcomes.

VI. REFERENCES

- Abbe, R. (1894). The surgery of the hand. *NY Med J*, 59, 33.
- Abrahamse, S., Dinant, S., Pfaffendorf, M., & Van Gulik, T. (2002). In vitro function of porcine carotid arteries preserved in UW, HTK and Celsior solutions. *Fundamental & clinical pharmacology*, 16(6), 503-511.
- Anderson, J. M., Rodriguez, A., & Chang, D. T. (2008). *Foreign body reaction to biomaterials*. Paper presented at the Seminars in immunology.
- Androsov, P. (1956). New method of surgical treatment of blood vessel lesions. *AMA archives of surgery*, 73(6), 902-910.
- Ang, E., Tan, K., Tan, L., Ng, R., & Song, I. (2001). 2-octylcyanoacrylate-assisted microvascular anastomosis: comparison with a conventional suture technique in rat femoral arteries. *Journal of reconstructive microsurgery*, 17(3), 193-201.
- Anyanwu, A. C., Fischer, G. W., Plotkina, I., Pinney, S., & Adams, D. H. (2007). Off-pump implant of the Jarvik 2000 ventricular assist device through median sternotomy. *The Annals of thoracic surgery*, 84(4), 1405-1407.
- Baker, D. M. D., M. (2015, 15/04/2015). Arteries. Retrieved April 21, 2016, from <http://clinicalgate.com/arteries-2/>

- Bar-El, Y., Tio, F. O., & Shofti, R. (2003). CorLink™ sutureless aortic anastomotic device: results of an animal study. *Journal of Surgical Research*, 115(1), 127-132.
doi: [http://dx.doi.org/10.1016/S0022-4804\(03\)00191-4](http://dx.doi.org/10.1016/S0022-4804(03)00191-4)
- Bartoli, C. R., Giridharan, G. A., Litwak, K. N., Sobieski, M., Prabhu, S. D., Slaughter, M. S., & Koenig, S. C. (2010). Hemodynamic responses to continuous versus pulsatile mechanical unloading of the failing left ventricle. *Asaio j*, 56(5), 410-416. doi: 10.1097/MAT.0b013e3181e7bf3c
- Baumgartner, B., Draxler, W., & Lewis, K. M. (2016). Treatment of Severe Aortic Bleeding Using Hemopatch in Swine on Dual Antiplatelet Therapy. *Journal of Investigative Surgery*, 1-9.
- Baumgartner, N., Dobrin, P. B., Morasch, M., Dong, Q.-S., & Mrkvicka, R. (1996). Influence of suture technique and suture material selection on the mechanics of end-to-end and end-to-side anastomoses. *The Journal of thoracic and cardiovascular surgery*, 111(5), 1063-1072.
- Berggren, A., Ostrup, L. T., & Lidman, D. (1987). Mechanical anastomosis of small arteries and veins with the unilink apparatus: a histologic and scanning electron microscopic study. *Plastic and reconstructive surgery*, 80(2), 274-283.
- Bergmann, L., Kottenberg-Assenmacher, E., & Peters, J. (2007). Management of a patient with right ventricular drainage cannula obstruction after biventricular assist device implantation. *Journal of cardiothoracic and vascular anesthesia*, 21(2), 262-264.
- Bergmann, P., Meszaros, K., Huber, S., Oberwalder, P., Machler, H., Schaffler, G., . . . Rigler, B. (2007). Forty-one-month follow-up of the Symmetry aortic connector

- system for proximal venous anastomosis. *J Thorac Cardiovasc Surg*, 134(1), 23-28. doi: 10.1016/j.jtcvs.2007.02.007
- Biancari, F., Lahtinen, J., Ojala, R., Ahvenjärvi, L., Jartti, A., Mosorin, M., . . . Lepojärvi, M. (2007). Spyder Aortic Connector System in Off-Pump Coronary Artery Bypass Surgery. *The Annals of thoracic surgery*, 84(1), 254-257. doi: <http://dx.doi.org/10.1016/j.athoracsur.2007.02.022>
- Birks, E. J. (2010). Left ventricular assist devices. *Heart*, 96(1), 63-71.
- Birks, E. J., Hall, J. L., Barton, P. J., Grindle, S., Latif, N., Hardy, J. P., . . . Miller, L. W. (2005). Gene profiling changes in cytoskeletal proteins during clinical recovery after left ventricular–assist device support. *Circulation*, 112(9 suppl), I-57-I-64.
- Birks, E. J., Tansley, P. D., Hardy, J., George, R. S., Bowles, C. T., Burke, M., . . . Yacoub, M. H. (2006). Left ventricular assist device and drug therapy for the reversal of heart failure. *New England Journal of Medicine*, 355(18), 1873-1884.
- Boening, A., Schoeneich, F., Lichtenberg, A., Bagaev, E., Cremer, J. T., & Klima, U. (2005). First clinical results with a 30 degrees end-to-side coronary anastomosis coupler. *Eur J Cardiothorac Surg*, 27(5), 876-881. doi: 10.1016/j.ejcts.2004.12.065
- Borgermann, J., Hakim, K., Renner, A., Parsa, A., Aboud, A., Becker, T., . . . Kuss, O. (2012). Clampless off-pump versus conventional coronary artery revascularization: a propensity score analysis of 788 patients. *Circulation*, 126(11 Suppl 1), S176-182. doi: 10.1161/circulationaha.111.084285
- Brumby, S., Petrucco, M., Walsh, J., & Bond, M. (1992). A RETROSPECTIVE ANALYSIS OF INFRA-INGUINAL ARTERIAL RECONSTRUCTION:

- THREE YEAR PATENCY RATES. *Australian and New Zealand Journal of Surgery*, 62(4), 256-260.
- Bruns, T. B., & Worthington, J. M. (2000). Using tissue adhesive for wound repair: a practical guide to dermabond. *American family physician*, 61(5), 1383-1388.
- Buijsrogge, M. P., Scheltes, J. S., Heikens, M., Gründeman, P. F., Pistecky, P. V., & Borst, C. (2002). Sutureless coronary anastomosis with an anastomotic device and tissue adhesive in off-pump porcine coronary bypass grafting. *The Journal of thoracic and cardiovascular surgery*, 123(4), 788-794.
- Callow, A. (1982). *Historical overview of experimental and clinical development of vascular grafts*. New York: Grune & Stratton.
- Carrel, A. (1902). La technique operatoire des anastomoses vasculaires et la transplantation des visceres. *Lyon Med*, 98, 859-863.
- Carton, C. A., Heifetz, M. D., & Kessler, L. A. (1962). Patching of Intracranial Internal Carotid Artery in Man Using a Plastic Adhesive (Eastman 910 Adhesive)*. *Journal of neurosurgery*, 19(10), 887-896.
- Carton, C. A., Kessler, L., Seidenberg, B., & Hurwitt, E. (1960). *Experimental studies in the surgery of small blood vessels. IV. Nonsuture anastomosis of arteries and veins, using flanged ring prostheses and plastic adhesive*. Paper presented at the Surgical forum.
- Carton, C. A., Kessler, L. A., Seidenberg, B., & Hurwitt, E. S. (1961). Experimental Studies in Surgery of Small Blood Vessels: II. Patching of Arteriotomy Using a Plastic Adhesive*. *Journal of neurosurgery*, 18(2), 188-194.

- Cheung, A., Lamarche, Y., Kaan, A., Munt, B., Doyle, A., Bashir, J., & Janz, P. (2011). Off-pump implantation of the HeartWare HVAD left ventricular assist device through minimally invasive incisions. *The Annals of thoracic surgery*, *91*(4), 1294-1296.
- Colvin-Adams, M., Smithy, J. M., Heubner, B. M., Skeans, M. A., Edwards, L. B., Waller, C., . . . Kasiske, B. L. (2014). OPTN/SRTR 2012 Annual Data Report: Heart. *American Journal of Transplantation*, *14*(S1), 113-138. doi: 10.1111/ajt.12583
- Cullen, M. E., Yuen, A. H., Felkin, L. E., Smolenski, R. T., Hall, J. L., Grindle, S., . . . Barton, P. J. (2006). Myocardial Expression of the Arginine: Glycine Amidinotransferase Gene Is Elevated in Heart Failure and Normalized After Recovery Potential Implications for Local Creatine Synthesis. *Circulation*, *114*(1 suppl), I-16-I-20.
- Dandel, M., Weng, Y., Siniawski, H., Potapov, E., Lehmkühl, H. B., & Hetzer, R. (2005). Long-term results in patients with idiopathic dilated cardiomyopathy after weaning from left ventricular assist devices. *Circulation*, *112*(9 suppl), I-37-I-45.
- Daniel, R. K., & Olding, M. (1984). An absorbable anastomotic device for microvascular surgery: experimental studies. *Plastic and reconstructive surgery*, *74*(3), 329-336.
- Detweiler, M. B., Detweiler, J. G., & Fenton, J. (1999). Sutureless and reduced suture anastomosis of hollow vessels with fibrin glue: a review. *Journal of Investigative Surgery*, *12*(5), 245-262.
- Dewey, T. M., Crumrine, K., Herbert, M. A., Leonard, A., Prince, S. L., Worley, C., . . . Mack, M. J. (2004). First-year outcomes of beating heart coronary artery bypass

grafting using proximal mechanical connectors. *The Annals of thoracic surgery*, 77(5), 1542-1549.

Dohmen, G., Hatam, N., Goetzenich, A., Mahnken, A., Autschbach, R., & Spillner, J. (2011). PAS-Port(R) clampless proximal anastomotic device for coronary bypass surgery in porcelain aorta. *Eur J Cardiothorac Surg*, 39(1), 49-52. doi: 10.1016/j.ejcts.2010.04.010

Eckstein, F. S., Bonilla, L. F., Englberger, L., Immer, F. F., Berg, T. A., Schmidli, J., & Carrel, T. P. (2002). The St Jude Medical symmetry aortic connector system for proximal vein graft anastomoses in coronary artery bypass grafting. *The Journal of thoracic and cardiovascular surgery*, 123(4), 777-782.

Elblbesy, M. A. (2014). Plasma viscosity and whole blood viscosity as diagnostic tools of blood abnormalities by using simple syringe method. *Medical Instrumentation*, 2(1), 5.

Ferrari, E., Tozzi, P., & von Segesser, L. K. (2007). The Vascular Join: a new sutureless anastomotic device to perform end-to-end anastomosis. Preliminary results in an animal model. *Interactive cardiovascular and thoracic surgery*, 6(1), 5-8.

Fillinger, M. F., Reinitz, E. R., Schwartz, R. A., Resetarits, D. E., Paskanik, A. M., Bruch, D., & Bredenberg, C. E. (1990). Graft geometry and venous intimal-medial hyperplasia in arteriovenous loop grafts. *Journal of vascular surgery*, 11(4), 556-566.

Frazier, O. (2003). Implantation of the Jarvik 2000 left ventricular assist device without the use of cardiopulmonary bypass. *The Annals of thoracic surgery*, 75(3), 1028-1030.

- Frazier, O., Benedict, C. R., Radovancevic, B., Bick, R. J., Capek, P., Springer, W. E., . . . Buja, L. M. (1996). Improved left ventricular function after chronic left ventricular unloading. *The Annals of thoracic surgery*, 62(3), 675-682.
- Frogel, J., Vodur, S., & Horak, J. (2008). Transesophageal echocardiography diagnosis of extracardiac left ventricular assist device inflow cannula obstruction in a patient with thoratec intracorporeal ventricular assist device biventricular support. *Journal of the American Society of Echocardiography*, 21(6), 777. e775-777. e776.
- Galvao, F. H., Bacchella, T., & Machado, M. C. (2007). Cuff-glue sutureless microanastomosis. *Microsurgery*, 27(4), 271-276. doi: 10.1002/micr.20354
- Giridharan, G. A., Koenig, S. C., Soucy, K. G., Choi, Y., Pirbodaghi, T., Bartoli, C. R., . . . Slaughter, M. S. (2015). Hemodynamic changes and retrograde flow in LVAD failure. *Asaio j*, 61(3), 282-291. doi: 10.1097/mat.0000000000000200
- Graf, K., Ott, E., Vonberg, R.-P., Kuehn, C., Haverich, A., & Chaberny, I. F. (2010). Economic aspects of deep sternal wound infections. *European Journal of Cardio-thoracic Surgery*, 37(4), 893-896.
- Gregoric, I. D., La Francesca, S., Myers, T., Cohn, W., Loyalka, P., Kar, B., . . . Frazier, O. (2008). A less invasive approach to axial flow pump insertion. *The Journal of Heart and Lung Transplantation*, 27(4), 423-426.
- Grubbs, P. E., Wang, S., Marini, C., Basu, S., Rose, D. M., & Cunningham, J. N. (1988). Enhancement of CO2 laser microvascular anastomoses by fibrin glue. *Journal of Surgical Research*, 45(1), 112-119.

- Gummert, J. F., Demertzis, S., Matschke, K., Kappert, U., Anssar, M., Siclari, F., . . . Harringer, W. (2006). Six-month angiographic follow-up of the PAS-Port II clinical trial. *The Annals of thoracic surgery*, 81(1), 90-96.
- Gummert, J. F., Opfermann, U., Jacobs, S., Walther, T., Kempfert, J., Mohr, F. W., & Falk, V. (2007). Anastomotic devices for coronary artery bypass grafting: technological options and potential pitfalls. *Computers in biology and medicine*, 37(10), 1384-1393.
- Hall, J. L., Birks, E. J., Grindle, S., Cullen, M. E., Barton, P. J., Rider, J. E., . . . Adhikari, N. (2007). Molecular signature of recovery following combination left ventricular assist device (LVAD) support and pharmacologic therapy. *European heart journal*, 28(5), 613-627.
- Harris, P. (1999). Haemodynamics of cuffed arterial anastomoses. *Critical ischaemia*, 9, 20-28.
- Hee Park, D., Bum Kim, S., Ahn, K. D., Yong Kim, E., Jun Kim, Y., & Keun Han, D. (2003). In vitro degradation and cytotoxicity of alkyl 2-cyanoacrylate polymers for application to tissue adhesives. *Journal of applied polymer science*, 89(12), 3272-3278.
- Heidenreich, P. A., Trogon, J. G., Khavjou, O. A., Butler, J., Dracup, K., Ezekowitz, M. D., . . . Khera, A. (2011). Forecasting the future of cardiovascular disease in the United States a policy statement from the American heart association. *Circulation*, 123(8), 933-944.
- Heilmann, C., Stahl, R., Schneider, C., Sukhodolya, T., Siepe, M., Olschewski, M., & Beyersdorf, F. (2013). Wound complications after median sternotomy: a single-

- centre study. *Interactive cardiovascular and thoracic surgery*, 16(5), 643-648.
doi: 10.1093/icvts/ivs554
- Huffmyer, J. L., & Groves, D. S. (2015). Pulmonary complications of cardiopulmonary bypass. *Best Pract Res Clin Anaesthesiol*, 29(2), 163-175. doi: 10.1016/j.bpa.2015.04.002
- Ikossi-O'Connor, M., Ambrus, J., & Rao, U. (1983). The role of fibrin adhesive in vascular surgery. *Journal of surgical oncology*, 23(3), 151-152.
- Jain, K., & Gorisch, W. (1979). Repair of small blood vessels with the neodymium-YAG laser: a preliminary report. *Surgery*, 85(6), 684-688.
- Jang, S., Yong, H. S., Doo, K. W., Kang, E. Y., Woo, O. H., & Choi, E. J. (2012). Relation of aortic calcification, wall thickness, and distensibility with severity of coronary artery disease: evaluation with coronary CT angiography. *Acta Radiol*, 53(8), 839-844. doi: 10.1258/ar.2012.110604
- Kai, M., Hanyu, M., Soga, Y., Nomoto, T., Nakano, J., Matsuo, T., . . . Okabayashi, H. (2009). Midterm patency rate after saphenous vein grafting with a PAS-Port device. *The Journal of thoracic and cardiovascular surgery*, 137(2), 503-504.
- Kaplon, R. J., Qi, X.-s., Andreopoulos, F. M., Anderson, M. B., Bauerlein, E., Nejman, A., & Pham, S. M. (2001). Tricuspid valvectomy for right ventricular outflow cannula occlusion with the Thoratec ventricular assist device. *The Journal of thoracic and cardiovascular surgery*, 121(4), 812-813.
- Kim, B.-Y., Choi, B.-H., Huh, J.-Y., Lee, S.-H., Zhu, S.-J., & Cho, B.-P. (2004). Microvascular anastomosis using cyanoacrylate adhesives. *Journal of reconstructive microsurgery*, 20(4), 317-321.

- Kirklin, J. K., Naftel, D. C., Pagani, F. D., Kormos, R. L., Stevenson, L. W., Blume, E. D., . . . Young, J. B. (2014). Sixth INTERMACS annual report: a 10,000-patient database. *The Journal of Heart and Lung Transplantation*, 33(6), 555-564.
- Kirklin, J. K., Naftel, D. C., Pagani, F. D., Kormos, R. L., Stevenson, L. W., Blume, E. D., . . . Young, J. B. (2015). Seventh INTERMACS annual report: 15,000 patients and counting. *The Journal of Heart and Lung Transplantation*, 34(12), 1495-1504.
- Kirsch, W. M. Z., YH; Whalstrom, E; Wang, ZG; Hardesty, R; Oberg, K. (1998). *Techniques in vascular and endovascular surgery*. Stamford, Connecticut: Appleton & Lange.
- Koenig, S. C., Jimenez, J. H., West, S. D., Sobieski, M. A., Choi, Y., Monreal, G., . . . Slaughter, M. S. (2014). Early Feasibility Testing and Engineering Development of a Sutureless Beating Heart Connector for Left Ventricular Assist Devices. *ASAIO journal*, 60(6), 617-625.
- Koenig, S. C., Woolard, C., Drew, G., Unger, L., Gillars, K., Ewert, D., . . . Pantalos, G. (2004). Integrated data acquisition system for medical device testing and physiology research in compliance with good laboratory practices. *Biomedical Instrumentation & Technology*, 38(3), 229-240.
- Kornowski, R., Hong, M. K., Tio, F. O., Bramwell, O., Wu, H., & Leon, M. B. (1998). In-Stent Restenosis: Contributions of Inflammatory Responses and Arterial Injury to Neointimal Hyperplasia. *Journal of the American College of Cardiology*, 31(1), 224-230. doi: 10.1016/S0735-1097(97)00450-6

- Küçükaksu, D. S., Akgül, A., Çağlı, K., & Taşdemir, O. (2000). Beneficial effect of BioGlue® surgical adhesive in repair of iatrogenic aortic dissection. *Texas Heart Institute Journal*, 27(3), 307.
- Lal, B. K., Hobson, R. W., Goldstein, J., Geohagan, M., Chakhtoura, E., Pappas, P. J., . . . Padberg, F. T. (2003). In-stent recurrent stenosis after carotid artery stenting: life table analysis and clinical relevance. *Journal of vascular surgery*, 38(6), 1162-1168.
- Lang, N., Pereira, M. J., Lee, Y., Friehs, I., Vasilyev, N. V., Feins, E. N., . . . Fabozzo, A. (2014). A blood-resistant surgical glue for minimally invasive repair of vessels and heart defects. *Science translational medicine*, 6(218), 218ra216-218ra216.
- Latif, N., Yacoub, M. H., George, R., Barton, P. J., & Birks, E. J. (2007). Changes in sarcomeric and non-sarcomeric cytoskeletal proteins and focal adhesion molecules during clinical myocardial recovery after left ventricular assist device support. *The Journal of Heart and Lung Transplantation*, 26(3), 230-235.
- LeMaire, S. A., Carter, S. A., Won, T., Wang, X., Conklin, L. D., & Coselli, J. S. (2005). The threat of adhesive embolization: BioGlue leaks through needle holes in aortic tissue and prosthetic grafts. *The Annals of thoracic surgery*, 80(1), 106-111.
- Lenneman, A. J., & Birks, E. J. (2014). Treatment strategies for myocardial recovery in heart failure. *Current treatment options in cardiovascular medicine*, 16(3), 1-9.
- Leva, C., & Engström, K. G. (2003). Flow resistance over technical anastomoses in relation to the angle of distal end-to-side connections. *Scandinavian Cardiovascular Journal*, 37(3), 165-171.

Levy, D., Kenchaiah, S., Larson, M. G., Benjamin, E. J., Kupka, M. J., Ho, K. K., . . .

Vasan, R. S. (2002). Long-term trends in the incidence of and survival with heart failure. *New England Journal of Medicine*, 347(18), 1397-1402.

Li, A. E., Kamel, I., Rando, F., Anderson, M., Kumbasar, B., Lima, J. A., & Bluemke, D.

A. (2004). Using MRI to assess aortic wall thickness in the multiethnic study of atherosclerosis: distribution by race, sex, and age. *American Journal of Roentgenology*, 182(3), 593-597.

Mahdavi, A., Ferreira, L., Sundback, C., Nichol, J. W., Chan, E. P., Carter, D. J., . . .

Ben-Joseph, E. (2008). A biodegradable and biocompatible gecko-inspired tissue adhesive. *Proceedings of the National Academy of Sciences*, 105(7), 2307-2312.

Maltais, S., Davis, M. E., & Haglund, N. (2014). Minimally invasive and alternative

approaches for long-term LVAD placement: the Vanderbilt strategy. *Annals of cardiothoracic surgery*, 3(6), 563.

Mamikonian, L. S., Mamo, L. B., Smith, P. B., Koo, J., Lodge, A. J., & Turi, J. L. (2014).

Cardiopulmonary bypass is associated with hemolysis and acute kidney injury in neonates, infants, and children*. *Pediatr Crit Care Med*, 15(3), e111-119. doi: 10.1097/pcc.0000000000000047

Marc, H. M., Mees, U., Hill, A., Egbert, B., Coker, G., & Estridge, T. (2000). *Evaluation*

of a novel synthetic sealant for inhibition of cardiac adhesions and clinical experience in cardiac surgery procedures. Paper presented at the The heart surgery forum.

- Mattox, D. E., & Wozniak, J. J. (1991). Sutureless vascular anastomosis with biocompatible heat-shrink tubing. *Archives of Otolaryngology–Head & Neck Surgery*, *117*(11), 1260-1264.
- Middleton, W. G., Matthews, W., & Chiasson, D. (1991). Histoacryl glue in microvascular surgery. *The Journal of otolaryngology*, *20*(5), 363-366.
- Mitrev, Z., Belostotskii, V., & Hristov, N. (2007). Suture line reinforcement using suction-assisted bioglue application during surgery for acute aortic dissection. *Interactive cardiovascular and thoracic surgery*, *6*(2), 147-149.
- Mozaffarian, D., Benjamin, E. J., Go, A. S., Arnett, D. K., Blaha, M. J., Cushman, M., . . . Howard, V. J. (2015). Heart disease and stroke statistics-2015 update: a report from the american heart association. *Circulation*, *131*(4), e29.
- Mueller, K.-M., & Dasbach, G. (1994). The pathology of vascular grafts *The Pathology of Devices* (pp. 273-306): Springer.
- Muir, E. (1914). A new device for anastomosing blood vessels. . *Lancet*, *34*, 211.
- Nakayama, K., Tamiya, T., Yamamoto, K., & Akimoto, S. (1962). A simple new apparatus for small vessel anastomosis (free autograft of the sigmoid included). *Surgery*, *52*(6), 918-931.
- Nitze, M. (1897). Kongress in Moskau. *Centralbl Chir*, *24*, 1042.
- Ohri, S. K., Desai, J. B., Gaer, J. A. R., Roussak, J. B., Hashemi, M., Smith, P. L. C., & Taylor, K. M. (1991). Intraabdominal complications after cardiopulmonary bypass. *The Annals of thoracic surgery*, *52*(4), 826-831. doi: [http://dx.doi.org/10.1016/0003-4975\(91\)91219-L](http://dx.doi.org/10.1016/0003-4975(91)91219-L)

- Ojha, M. (1994). Wall shear stress temporal gradient and anastomotic intimal hyperplasia. *Circulation Research*, 74(6), 1227-1231.
- Payr, E. (1904). Zur Frage der zirkularen Vereinigung von Blutgefäße mit resorbierbaren Prothesen. *Arch Klein Chir*, 62, 67-93.
- Perrin, B. R., Dupeux, M., Tozzi, P., Delay, D., Gersbach, P., & von Segesser, L. K. (2009). Surgical glues: are they really adhesive? *European Journal of Cardio-thoracic Surgery*, 36(6), 967-972.
- Phillips, A., Ginsburg, B. Y., Shin, S. J., Soslow, R., Ko, W., & Poppas, D. P. (1999). Laser welding for vascular anastomosis using albumin solder: An approach for MID-CAB. *Lasers in surgery and medicine*, 24(4), 264-268.
- Puskas, J. D., Halkos, M. E., Balkhy, H., Caskey, M., Connolly, M., Crouch, J., . . . Matschke, K. (2009). Evaluation of the PAS-Port Proximal Anastomosis System in coronary artery bypass surgery (the EPIC trial). *The Journal of thoracic and cardiovascular surgery*, 138(1), 125-132. doi: <http://dx.doi.org/10.1016/j.jtcvs.2009.02.017>
- Riess, F.-C., Helmold, H., Hilfer, I., Bader, R., Stripling, J., Loewer, C., . . . Bleese, N. (2002). *Clinical experience with the CorLink device for proximal anastomosis of the saphenous vein to the aorta: a clinical, prospective, and randomized study.* Paper presented at the HEART SURGERY FORUM.
- Roger, Go, A. S., Lloyd-Jones, D. M., Benjamin, E. J., Berry, J. D., Borden, W. B., . . . Turner, M. B. (2012). Heart disease and stroke statistics--2012 update: a report from the American Heart Association. *Circulation*, 125(1), e2-e220. doi: 10.1161/CIR.0b013e31823ac046

- Roger, V. L., Weston, S. A., Redfield, M. M., Hellermann-Homan, J. P., Killian, J., Yawn, B. P., & Jacobsen, S. J. (2004). Trends in heart failure incidence and survival in a community-based population. *Jama*, 292(3), 344-350.
- Rojas, S. V., Avsar, M., Hanke, J. S., Khalpey, Z., Maltais, S., Haverich, A., & Schmitto, J. D. (2015). Minimally invasive ventricular assist device surgery. *Artificial organs*, 39(6), 473-479.
- Rose, E. A., Gelijns, A. C., Moskowitz, A. J., Heitjan, D. F., Stevenson, L. W., Dembitsky, W., . . . Levitan, R. G. (2001). Long-term use of a left ventricular assist device for end-stage heart failure. *New England Journal of Medicine*, 345(20), 1435-1443.
- Rylski, B., Desjardins, B., Moser, W., Bavaria, J. E., & Milewski, R. K. (2014). Gender-related changes in aortic geometry throughout life. *Eur J Cardiothorac Surg*, 45(5), 805-811. doi: 10.1093/ejcts/ezt597
- Sacak, B., Tosun, U., Egemen, O., Sakiz, D., & Ugurlu, K. (2015). Microvascular anastomosis using fibrin glue and venous cuff in rat carotid artery. *J Plast Surg Hand Surg*, 49(2), 72-76. doi: 10.3109/2000656x.2013.800528
- Saha, S. P., Muluk, S., Schenk, W., Dennis, J. W., Ploder, B., Grigorian, A., . . . Goppelt, A. (2012). A prospective randomized study comparing fibrin sealant to manual compression for the treatment of anastomotic suture-hole bleeding in expanded polytetrafluoroethylene grafts. *Journal of vascular surgery*, 56(1), 134-141.
- Scheltes, J. S., Heikens, M., Pistecky, P. V., van Andel, C. J., & Borst, C. (2000). Assessment of patented coronary end-to-side anastomotic devices using micromechanical bonding. *The Annals of thoracic surgery*, 70(1), 218-221.

- Sergeant, P., Kocharian, R., Patel, B., Pfefferkorn, M., & Matonick, J. (2016). Needle-to-suture ratio, as well as suture material, impacts needle-hole bleeding in vascular anastomoses. *Interactive cardiovascular and thoracic surgery*, ivw042.
- Shiia, N., Kunihara, T., Matsuzaki, K., & Sugiki, T. (2006). Spontaneous perigraft hematoma suggesting transgraft hemorrhage seven years after thoracic aortic replacement with a Dacron graft. *European Journal of Cardio-thoracic Surgery*, 30(2), 402-404.
- Slaughter, M. S., Rogers, J. G., Milano, C. A., Russell, S. D., Conte, J. V., Feldman, D., . . . Long, J. W. (2009). Advanced heart failure treated with continuous-flow left ventricular assist device. *New England Journal of Medicine*, 361(23), 2241-2251.
- Stanger, O., Oberwalder, P., Dacar, D., Knez, I., & Rigler, B. (2002). Late dissection of the ascending aorta after previous cardiac surgery: risk, presentation and outcome. *European Journal of Cardio-thoracic Surgery*, 21(3), 453-458.
- Stehlik, J., Edwards, L. B., Kucheryavaya, A. Y., Aurora, P., Christie, J. D., Kirk, R., . . . Hertz, M. I. (2010). The Registry of the International Society for Heart and Lung Transplantation: Twenty-seventh official adult heart transplant report—2010. *The Journal of Heart and Lung Transplantation*, 29(10), 1089-1103. doi: <http://dx.doi.org/10.1016/j.healun.2010.08.007>
- Stemper, B. D., Yoganandan, N., Stineman, M. R., Gennarelli, T. A., Baisden, J. L., & Pintar, F. A. (2007). Mechanics of Fresh, Refrigerated, and Frozen Arterial Tissue. *Journal of Surgical Research*, 139(2), 236-242. doi: <http://dx.doi.org/10.1016/j.jss.2006.09.001>

- Sun, B. C., Firstenberg, M. S., Louis, L. B., Panza, A., Crestanello, J. A., Sirak, J., & Sai-Sudhakar, C. B. (2008). Placement of long-term implantable ventricular assist devices without the use of cardiopulmonary bypass. *The Journal of Heart and Lung Transplantation*, 27(7), 718-721.
- Szanka, I., Szanka, A., Şen, S., Nugay, N., & Kennedy, J. P. (2015). Rubbery wound closure adhesives. I. design, synthesis, characterization, and testing of polyisobutylene-based cyanoacrylate homo-and co-networks. *Journal of Polymer Science Part A: Polymer Chemistry*.
- Takenaka, H., Esato, K., Ohara, M., & Zempo, N. (1992). Sutureless anastomosis of blood vessels using cyanoacrylate adhesives. *Surgery today*, 22(1), 46-54.
- Taylor, A. H., Mitchell, A. E., & Mitchell, I. M. (2012). A 15-year study of the changing demographics and infection risk in a new UK cardiac surgery unit. *Interactive cardiovascular and thoracic surgery*, 15(3), 390-394.
- Tozzi, Hayoz, Mueller, M'Baku, Mallabiabarrena, & Segesser, v. (2000a). Anastomotic longitudinal stress due to modification of arterial longitudinal properties after anastomosis. *Swiss Surgery*, 6(2), 74-76.
- Tozzi, Hayoz, Mueller, M'Baku, Mallabiabarrena, & Segesser, v. (2000b). Decreased compliance on arterial anastomoses. *Swiss Surgery*, 6(2), 77-79.
- Tozzi, P. (2007). *Sutureless Anastomoses: Secrets for Success*. Germany: Steinkopff Verlag Darmstadt.
- Traverse, J. H., Mooney, M. R., Pedersen, W. R., Madison, J. D., Flavin, T. F., Kshetry, V. R., . . . Emery, R. W. (2003). Clinical, angiographic, and interventional follow-

- up of patients with aortic-saphenous vein graft connectors. *Circulation*, 108(4), 452-456.
- Tuffier, M. (1915). De l'untubation dans les plaies des grosses arteries. *Bull Acad Natl Med*, 74, 455.
- Van Damme, H., Deprez, M., Creemers, E., & Limet, R. (2005). Intrinsic Structural Failure of Polyester (Dacron) Vascular Grafts. A General. *Acta chir belg*, 105, 249-255.
- Verberkmoes, N. J., Wolters, S. L., Post, J. C., Soliman-Hamad, M. A., ter Woorst, J. F., & Berreklouw, E. (2013). Distal anastomotic patency of the Cardica C-PORT(R) xA system versus the hand-sewn technique: a prospective randomized controlled study in patients undergoing coronary artery bypass grafting. *Eur J Cardiothorac Surg*, 44(3), 512-518; discussion 518-519. doi: 10.1093/ejcts/ezt079
- Wagner, C. E., Bick, J. S., Kennedy, J., Haglund, N., Danter, M., Davis, M. E., . . . Maltais, S. (2015). Minimally invasive thoracic left ventricular assist device implantation; case series demonstrating an integrated multidisciplinary strategy. *Journal of cardiothoracic and vascular anesthesia*, 29(2), 271-274.
- Walsh, M., Kavanagh, E., O'brien, T., Grace, P., & McGloughlin, T. (2003). On the existence of an optimum end-to-side junctional geometry in peripheral bypass surgery—a computer generated study. *European Journal of Vascular and Endovascular Surgery*, 26(6), 649-656.
- Weitzel, N., Puskas, F., Cleveland, J., Levi, M. E., & Seres, T. (2009). Left Ventricular Assist Device Outflow Cannula Obstruction by the Rare Environmental Fungus

- Myceliophthora thermophila. *Anesthesia & Analgesia*, 108(1), 73-75. doi:
10.1213/ane.0b013e318187b8fc
- Wille, T., de Groot, H., & Rauwen, U. (2008). Improvement of the cold storage of blood vessels with a vascular preservation solution. Study in porcine aortic segments. *Journal of vascular surgery*, 47(2), 422-431. doi:
<http://dx.doi.org/10.1016/j.jvs.2007.09.048>
- Williams, D. F. (2008). On the mechanisms of biocompatibility. *Biomaterials*, 29(20), 2941-2953.
- Zamvar, V., Williams, D., Hall, J., Payne, N., Cann, C., Young, K., . . . Dunne, J. (2002). Assessment of neurocognitive impairment after off-pump and on-pump techniques for coronary artery bypass graft surgery: prospective randomised controlled trial. *Bmj*, 325(7375), 1268.
- Zhang, L., Moskovitz, M., Piscatelli, S., Longaker, M. T., & Siebert, J. W. (1995). Hemodynamic study of different angled end-to-side anastomoses. *Microsurgery*, 16(2), 114-117.
- Zucchetta, F., Tarzia, V., Bottio, T., & Gerosa, G. (2014). The Jarvik-2000 ventricular assist device implantation: how we do it. *Annals of cardiothoracic surgery*, 3(5), 525-531.

APPENDIX I: RAW AND ADDITIONAL DATA

Table 8: Static pressure test raw leak rate data.

Pressure (mmHg)	Leak Rate (mL/30s)					
	Vessel 1		Vessel 2		Vessel 3	
	Leak Rate (mL/30s)	Note	Leak Rate (mL/30s)	Note	Leak Rate (mL/30s)	Note
0	0	Drip	0	Drip	0	Drip
50	0.6	Drip	7.8	Drip	0	Drip
100	1.6	Drip	14	Drip (Graft)	2.2	Drip
150	3.8	Drip	26	Drip (Graft)	4.2	Drip
200	5.4	Drip	32	Drip (Graft)	28	Drip (graft)

Table 9: Dynamic pressure test leak rate raw data.

Dynamic Pressure Leak Rate Data						
	Vessel 1		Vessel 2		Vessel 3	
	Leak Rate (mL/30s)	Note	Leak Rate (mL/30s)	Note	Leak Rate (mL/30s)	Note
Normal	5.6	Drip	17	Drip (graft)	10.5	Drip
Hypertension	5.7	Drip	18	Drip (graft)	11	Drip
Heart Failure	6.8	Drip	12.6	Drip (graft)	5.2	Drip
Partial VAD Support	7.9	Drip	11	Drip (graft)	5.7	Drip

Table 10: Dynamic pressure test hemodynamic beat-to-beat raw calculations

	Dynamic Pressure Hemodynamic Beat-to-Beat Data																							
	Normal					Hypertension					Heart Failure													
	1			2		3			1			2		3			1			2		3		
	Mean	SD		Mean	SD	Mean	SD		Mean	SD	Mean	SD		Mean	SD	Mean	SD		Mean	SD	Mean	SD		Mean
ArtPsys (mmHg)	119.7619	122.4282	121.1913	121.13	1.09	153.5128	150.0027	154.6328	152.72	2.42	95.2426	97.0879	90.0558	94.13	3.65	95.8218	94.3037	105.652	98.59	6.16				
ArtPdia (mmHg)	79.937	84.7091	80.9522	81.87	2.05	108.7969	114.9775	109.9676	111.25	3.28	64.5176	68.0929	63.353	65.32	2.47	62.9104	64.8212	72.7795	66.84	5.23				
Artm (mmHg)	100.1123	102.7337	99.1709	100.67	1.51	130.3919	131.8714	130.3163	130.86	0.88	78.6579	82.8376	75.775	79.09	3.55	78.9116	79.4807	91.3306	83.24	7.01				
AoPsys (mmHg)	156.4987	175.6651	130.615	154.26	18.46	191.8276	209.0879	161.1991	187.37	24.25	131.7895	148.44	100.5245	126.92	24.33	163.2917	184.416	132.669	160.13	26.02				
AoPdia (mmHg)	60.217	57.4825	73.8567	63.85	7.16	79.4422	73.0096	98.1111	83.52	13.04	34.7571	48.9852	47.9365	43.89	7.93	40.2696	48.8792	74.7618	54.64	17.95				
AoPm (mmHg)	108.2612	123.2161	104.3582	111.95	8.13	139.6164	153.6071	135.0574	142.76	9.67	83.7271	96.6912	78.6808	86.37	9.29	100.8563	116.2664	100.6235	105.92	8.96				
AoFsys (L/min)	4.6438	15.4334	20.7687	13.62	6.71	4.6316	15.6541	19.0216	13.10	7.53	3.6332	13.4689	17.3532	11.49	7.07	4.0487	12.859	14.7404	10.55	5.71				
AoFdia (L/min)	4.5453	-1.1502	-1.4496	0.65	2.76	4.5116	-1.4528	-1.4766	0.53	3.45	3.539	-1.059	-0.934	0.52	2.62	3.9461	-0.917	-1.2226	0.60	2.90				
AoFm (L/min)	4.5974	4.894	4.8871	4.79	0.14	4.5571	4.7672	4.6943	4.67	0.11	3.5849	3.4992	3.8654	3.65	0.19	3.9903	4.1517	4.1245	4.09	0.09				
VADFsys (L/min)	-0.0032	-0.0044	-0.0044	0.00	0.00	-0.0034	-0.0045	-0.0047	0.00	0.00	-0.003	-0.0046	-0.0045	0.00	0.00	2.8105	6.2365	7.7026	5.58	2.51				
VADFdia (L/min)	-0.0053	-0.0062	-0.0061	-0.01	0.00	-0.0055	-0.0062	-0.0063	-0.01	0.00	-0.0051	-0.0063	-0.0061	-0.01	0.00	2.7517	-2.499	-2.9211	-0.89	3.16				
VADFm (L/min)	-0.0043	-0.0053	-0.0053	0.00	0.00	-0.0045	-0.0053	-0.0055	-0.01	0.00	-0.0041	-0.0054	-0.0053	0.00	0.00	2.7804	2.3637	2.3127	2.49	0.26				

Table 11: Pull-out force raw Data.

	Peak Pull-out Strength (N)	
	Device	Suture
1	63.43	53.43
2	31.62	67.95
3	35.66	69.06

APPENDIX II: STATISTICAL ANALYSIS

A) Dynamic Pressure Leak Rate ANOVA

Table Analyzed Data 1

ANOVA summary

F 0.4194

P value 0.7441

P value summary ns

Are differences among means statistically significant? (P < 0.05) No

R square 0.1359

Brown-Forsythe test

F (DFn, DFd) 0.4021 (3, 8)

P value 0.7555

P value summary ns

Significantly different standard deviations? (P < 0.05) No

Bartlett's test

Bartlett's statistic (corrected)

P value

P value summary

Significantly different standard deviations? (P < 0.05)

ANOVA table	SS	DF	MS	F (DFn, DFd)	P value	
Treatment (between columns)				117.0 3	39.01	F (3, 8) = 0.4194 P =
Residual (within columns)			744.1	8	93.02	
Total	861.2	11				

Data summary

Number of treatments (columns) 4

Number of values (total) 12

B) Unpaired ANOVA against Literature Data

Table Analyzed Data 1

ANOVA summary

F 83.02

P value < 0.0001

P value summary ****

Are differences among means statistically significant? (P < 0.05) Yes

R square 0.8098

Brown-Forsythe test

F (DFn, DFd)

P value

P value summary

Significantly different standard deviations? (P < 0.05)

Bartlett's test

Bartlett's statistic (corrected)

P value

P value summary

Significantly different standard deviations? (P < 0.05)

ANOVA table	SS	DF	MS	F (DFn, DFd)	P value
Treatment (between columns)	16516	4	4129	F (4, 78) = 83.02	P < 0.0001
Residual (within columns)	3879	78	49.73		
Total	20395	82			

Data summary

Number of treatments (columns) 5

Number of values (total) 83

B) Tukey Test of Leak Rates from Device vs Literature

Number of families 1
 Number of comparisons per family 10
 Alpha 0.05

Tukey's multiple comparisons test Summary	Mean Diff.	95% CI of diff.	Significant?
Device vs. SH	2.270	-9.923 to 14.46	No ns A-B
Device vs. PR 1	-35.13	-47.32 to -22.94	Yes **** A-C
Device vs. PR 2	-11.73	-23.92 to 0.4635	No ns A-D
Device vs. PTFE	-24.43	-36.62 to -12.24	Yes **** A-E
SH vs. PR 1	-37.40	-43.63 to -31.17	Yes **** B-C
SH vs. PR 2	-14.00	-20.23 to -7.772	Yes **** B-D
SH vs. PTFE	-26.70	-32.93 to -20.47	Yes **** B-E
PR 1 vs. PR 2	23.40	17.17 to 29.63	Yes **** C-D
PR 1 vs. PTFE	10.70	4.472 to 16.93	Yes **** C-E
PR 2 vs. PTFE	-12.70	-18.93 to -6.472	Yes **** D-E

Test details	Mean 1	Mean 2	Mean Diff.	SE of diff.	n1	n2		
q	DF							
Device vs. SH	22.07	19.80	2.270	4.366	3	20	0.7352	78
Device vs. PR 1	22.07	57.20	-35.13	4.366	3	20	11.38	78
Device vs. PR 2	22.07	33.80	-11.73	4.366	3	20	3.799	78
Device vs. PTFE	22.07	46.50	-24.43	4.366	3	20	7.913	78
SH vs. PR 1	19.80	57.20	-37.40	2.230	20	20	23.72	78
SH vs. PR 2	19.80	33.80	-14.00	2.230	20	20	8.878	78
SH vs. PTFE	19.80	46.50	-26.70	2.230	20	20	16.93	78
PR 1 vs. PR 2	57.20	33.80	23.40	2.230	20	20	14.84	78
PR 1 vs. PTFE	57.20	46.50	10.70	2.230	20	20	6.785	78
PR 2 vs. PTFE	33.80	46.50	-12.70	2.230	20	20	8.054	78

C) Paired T-Test for Pull-Out Tests

Table Analyzed Paired t test data

Column A Device

vs. vs.

Column B Suture

Paired t test

P value 0.3151

P value summary ns

Significantly different? ($P < 0.05$) No

One- or two-tailed P value? Two-tailed

t, df $t=1.329$ $df=2$

Number of pairs 3

How big is the difference?

Mean of differences -19.91

SD of differences 25.94

SEM of differences 14.98

95% confidence interval -84.36 to 44.54

R squared 0.4690

How effective was the pairing?

Correlation coefficient (r) -0.9837

P value (one tailed) 0.0575

P value summary ns

Was the pairing significantly effective? No

VII. Curriculum Vitae

YOUNG CHOI

MEng Student in Bioengineering
J.B. Speed School of Engineering
University of Louisville

Education:

Master of Engineering in Bioengineering | University of Louisville | Expected 2015 | GPA 3.79 / 4.00
Bachelor of Science in Bioengineering *with Honors* | University of Louisville | 2014 | GPA 3.26 / 4.00

Contact:

(502) 938-3231
y0choi05@louisville.edu
1021 Ardmore Drive
Louisville, KY 40217

Office:

Cardiovascular Innovation Institute
302 East Muhammad Ali Blvd.
Department of Bioengineering
University of Louisville
Louisville, KY 40202
Fax: 502-587-4011

Academic and Professional Experience:

Research Assistant | Cardiovascular Innovation Institute | May 2014 – Present

- Support principal investigators of the Cardiovascular Research (CARE) group with data acquisition, and grant/manuscript preparation
- Develop a device for sutureless left ventricular assist device outflow graft anastomosis as Master's of Engineering (MEng) thesis

- Perform weekly echocardiography assessment using a Philips IE33 Ultrasound System of large animals with mechanical circulatory support devices implanted

Engineering Co-op | Cardiovascular Innovation Institute | Aug 2012 – May 2014

- Provided engineering support through data instrumentation, acquisition and analysis, developing experimental protocols, and grant/manuscript writing
- Captured intraoperative echocardiograms using a Philips IE33 Ultrasound System during large animal studies, and performed 3-D volumetric analysis using QLAB quantification software (Philips, Amsterdam, Netherlands)
- Assisted in large animal and cadaver studies for mechanical circulatory support devices and medical devices as engineering support and circulator
- Designed Solidworks (Dassault Systèmes SolidWorks Corp., Waltham, MA) computer-aided designs (CADs) of electrocardiogram (EKG) leads and cannulas; EKG leads were prototyped
- Generated signal processing MATLAB scripts for reduction and analysis of hemodynamic waveform data
- Supervised a high school student's Intel International Science and Engineering Fair (ISEF) project – Sumanth Chenraddy
- Designed and conducted ex-vivo experiments with kidneys and carotid arteries investigating pulsatility effects

Clinical Research Associate | University Cardiothoracic Surgical Associates, Jewish Hospital Rudd Heart and Lung Center | Jan 2013 – Jan 2014

- HIPAA certified for data and tissue collection, and retrieval of informed patient consent for clinical research studies
- Harvested and processed tissue for multiple Institutional Review Board (IRB) approved clinical studies
- Compiled retrospective data on 180+ patients from patient medical records for multi-institutional study in cooperation with Natasha Loghmanpour (Carnegie-Mellon University) to develop a risk stratification model for ventricular assist device 90-day survival
- Retrieved and input data for IRB studies involving ventricular assist device implantation; devices included HVAD (HeartWare International Inc., Framingham, MA) and HeartMate II (Thoratec Corp., Pleasanton, CA) Ventricular Assist Devices

Bachelors of Science Senior Capstone Project | University of Louisville | Aug 2013 – Dec 2013

- Worked on a team to develop MATLAB code for body edge detection in Multi-Spectral Optoacoustic Tomography (MSOT) images, including a complete mock FDA 510(k) submission for market approval
- Independently generated Matlab code for Region of Interest (ROI) masking of MSOT color images for Dr. Lacey McNally at the James Graham Brown Cancer Center

Student Research Assistant | University of Louisville | Feb 2012 – Dec 2012

- Conducted background research for the development of 3-dimensional cellular models of ovarian cancer under the supervision of Dr. Hermann B Frieboes

Technical Skills:

- Software: MATLAB (Signal/Image Processing), ANSYS, LabVIEW, Multisim, SolidWorks, AutoCAD, Adobe Photoshop CS6, Microsoft Office, Minitab, GraphPad Prism, Phillips QLAB
- Programming: C++, HTML (CSS), Android Studio, Arduino
- Languages: Korean (advanced, 10+ years studied), Spanish (advanced, 13+ years studied), German (beginner, 1 year studied)

Leadership Positions and Activities:

Biomedical Engineering Society Louisville Student Chapter | President May 2014 – Sept 2014 |

Member Jan 2014 - Present

- Fundraised \$3000+ for the organization that was used for BMES events on campus and cover travel expenses for 3 undergraduate BMES members to attend the 2014 BMES Annual Meeting in San Antonio, TX
- Organized the 3rd Annual Bioengineering Pig Roast and Research Showcase—An annual BMES event at the University of Louisville to showcase the Bioengineering departmental research to student body

Biomedical Engineering Society (BMES) | Member 2014 to 2015**American Society of Artificial Internal Organs (ASAIO) | Member Aug 2014 - Present**

- Attended the ASAIO 60th-61st Annual Conference

Biomedical Engineering Society**Bamboozle Breakdance Crew | Member Jan 2010 – Present**

- Perform as part of a dance group at local venues, events, and fundraisers
- Instruct classes at Saffiyah's Dance Company (Louisville, KY)

Americana Community Center Volunteer | May 2010 – Dec 2011

- Founding member of the student organization intended to promote dance within the Louisville community as a fun and safe activity for young adults
- Volunteered weekly at the Americana Community Center, Inc. (Louisville, KY) to provide free dance classes to low-income families, including refugees and immigrants

Honors:**Whitaker International Fellow**

Award funding one year abroad for the development of a right ventricular assist device at RWTH Aachen University (Aachen, Germany)

Joseph Henry Award in Translational Bioengineering

Award recognizing a student who has devised or potentially devised a new medical invention

Rolando “Chip” Cheng, Jr. Memorial Scholarship

Award recognizing a student that reflects humanitarianism, innovative mind, and entrepreneurial spirit.”

Master of Engineering (MEng) Research Assistantship

MEng scholarship that provides full tuition plus stipend graduate studies sponsored by Dr. Steven Koenig

Trustee's Scholarship

Competitive undergraduate scholarship that provides full tuition.

Kentucky Educational Excellence Scholarship (KEES) Award

Scholarship award that provided up to \$2225 each academic year for four years based on high school GPA, ACT score, and Advanced Placement course credit.

Additional Honors & Awards

- Dean's List (Spring 2012, Summer 2012, Fall 2013)
- University of Louisville Honor's Program

Peer Reviewed Publications:

Peer-Reviewed Journals - Published

1. Linsky PL, Choi Y, Ouseph R, Slaughter MS, Keller BB, Jones CM. High Resolution Imaging using the VisualSonics Vevo 2100 on Isolated, Perfused Porcine Kidneys on Mechanical Circulatory Support. *ASAIO J.* 2014;60(4):473-8.
2. Koenig SC, Jimenez JH, West SD, Sobieski MA, Choi Y, Monreal G, Giridharan GA, Soucy KG, Slaughter MS. Early Feasibility Testing and Engineering Development of a Universal Sutureless Beating Heart (SBH) Connector for Left Ventricular Assist Devices (LVAD). *ASAIO J.* 2014;60(6):617-25.
3. Slaughter MS, Soucy KG, Matheny RG, Lewis BC, Hennick MF, Choi Y, Monreal G, Sobieski MA, Giridharan GA, Koenig SC. Development of an Extracellular Matrix (ECM) Delivery System for Effective Intramyocardial Injection in Ischemic Tissue. *ASAIO J.* 2014;60(6):730-6.
4. Soucy KG, Giridharan GA, Choi Y, Sobieski MA, Monreal G, Schumer E, Slaughter MS, Koenig SC. Rotary Pump Speed Modulation for Generating Pulsatile Flow and Phasic Left Ventricular Volume Unloading in a Bovine Model of Chronic Ischemic Heart Failure. *J Heart Lung Transplant.* 2015;34(1):122-31.
5. Giridharan GA, Koenig SC, Soucy KG, **Choi Y**, Pirbodaghi T, Bartoli CR, Monreal G, Sobieski MA, Schumer E, Cheng A, Slaughter MS. Hemodynamic Changes and Retrograde Flow in LVAD Failure. *ASAIO J.* 2015;61(3):282-91.
6. Giridharan GA, Koenig SC, Soucy KG, **Choi Y**, Pirbodaghi T, Bartoli CR, Monreal G, Sobieski MA, Schumer E, Cheng A, Slaughter MS. Left Ventricular Volume Unloading with Axial and Centrifugal Rotary Blood Pumps. *ASAIO J.* 2015;61(3):292-300.
7. Schumer EM, Zoeller KA, Linsky PL, Monreal G, **Choi Y**, Giridharan GA, Sobieski MA, Slaughter MS, van Berkel VH. Feasibility study of pulsatile left ventricular assist device for prolonged ex vivo lung perfusion. *Annals of Thoracic Surgery.* 2015;99(6):1961-7.